



Review article

Rodent models of pulmonary embolism and chronic thromboembolic pulmonary hypertension



Andrei A. Karpov^{a,b,*}, Dariya D. Vaulina^a, Sergey S. Smirnov^a, Olga M. Moiseeva^a, Michael M. Galagudza^{a,**}

^a Almazov National Medical Research Centre, 197341 St. Petersburg, Russia

^b Saint Petersburg State Chemical Pharmaceutical University, 197376 St. Petersburg, Russia

ARTICLE INFO

Keywords:

Pulmonary embolism
Chronic thromboembolic pulmonary hypertension
Animal model
Mice
Rats
Rabbits

ABSTRACT

Pulmonary embolism (PE) is the third most prevalent cardiovascular disease. It is associated with high in-hospital mortality and the development of acute and chronic complications. New approaches aimed at improving the prognosis of patients with PE are largely dependent on reliable animal models. Mice, rats, hamsters, and rabbits, are currently most commonly used for PE modeling because of their ethical acceptability and economic feasibility. This article provides an overview of the main approaches to PE modeling, and the advantages and disadvantages of each method. Special attention is paid to experimental endpoints, including morphological, functional, and molecular endpoints. All approaches to PE modeling can be broadly divided into three main groups: 1) induction of thromboembolism, either by thrombus formation *in vivo* or by injection of *in vitro* prepared blood clots; 2) introduction of particles of non-thrombotic origin; and 3) surgical procedures. The choice of a specific model and animal species is determined based on the objectives of the study. Rodent models of chronic thromboembolic pulmonary hypertension (CTEPH), which is the most devastating complication of PE, are also described. CTEPH models are especially challenging because of insufficient knowledge about the pathogenesis and high fibrinolytic activity of rodent plasma. The CTEPH model should demonstrate a persistent increase in pulmonary artery pressure and stable reduction of the vascular bed due to recurrent embolism. Based on the analysis of available evidence, one might conclude that currently, there is no single optimal method for modeling PE and CTEPH.

1. Introduction

Pulmonary embolism (PE) is the third most common cardiovascular disease [1]. It is associated with high in-hospital mortality and the development of acute and chronic complications [2]. Moreover, observational studies have shown a trend towards an increase in the number of PE cases per year over time [3]. According to Keller et al. [4], the incidence of PE in Germany from 2005 to 2015 increased from 85 to 109 cases per 100 000 people per year. Similar data were obtained from the Danish National Patient Register, in which there was an increase in the incidence of PE between 2004 and 2014, from 45 to 83 cases per 100 000 people per year [5]. This trend may be accounted for by an increase in life expectancy, a greater prevalence of risk factors for PE, and a significant improvement in PE detection. In addition, PE can be accompanied by a number of complications. One of the most serious complications is

chronic thromboembolic pulmonary hypertension (CTEPH), which is characterized by incomplete lysis of thromboemboli and a sustained increase in pulmonary artery pressure. The five-year survival rate of patients with CTEPH receiving only oral anticoagulant therapy, with a mean pulmonary artery pressure of more than 30 mmHg, does not exceed 10% [6].

The treatment and prevention of PE, as well as its complications, require high-tech approaches aimed at improving patient prognosis. In this regard, experimental studies aimed at clarifying the pathogenesis, improving diagnostic methods, and identifying new drug targets for prevention and treatment of PE and its complications represent an unmet clinical need. Considering the current trends in preclinical research, the use of rodent models, such as mice, rats, hamsters, and rabbits is becoming more widespread. The use of these animal species is ethically acceptable and economically feasible.

* Corresponding author.

** Corresponding author.

E-mail addresses: karpovmed@gmail.com (A.A. Karpov), galagoudza@mail.ru (M.M. Galagudza).

<https://doi.org/10.1016/j.heliyon.2022.e09014>

Received 10 September 2021; Received in revised form 6 November 2021; Accepted 21 February 2022

2405-8440/© 2022 The Authors. Published by Elsevier Ltd. This is an open access article under the CC BY-NC-ND license (<http://creativecommons.org/licenses/by-nc-nd/4.0/>).

The literature describes a large number of models used to induce PE. All available approaches to modeling PE can be divided into three main groups:

- Induction of thromboembolism
 - Induction of thrombus formation in vivo
 - Injection of blood clots prepared in vitro
- Introduction of non-thrombotic particles
- Surgical procedures.

A separate direction in this area is the modeling of CTEPH. Due to the complex pathogenesis of this condition, as well as the high fibrinolytic activity of blood plasma in rodents, modeling this pathology is difficult and currently does not have an optimal solution.

The choice of animal species and the approach to modeling PE are primarily determined by the objectives of the specific study. This article provides an overview of the main approaches to the modeling of PE and discusses the advantages and disadvantages of each method. This study analyzed publications from 1978 to 2021, in which PE was induced in rodents.

2. PE modeling using thrombosis induction in vivo

For PE modeling by inducing endogenous thrombus formation, animals are injected intravenously with agonists causing platelet aggregation or substances that trigger the coagulation cascade. Table 1 summarizes the studies performed using these models. This group of models is most often used to study the anticoagulant [7, 8, 9] and antiplatelet [10, 11, 12] activity of pharmacological substances, and to investigate the pathogenesis of various forms of blood coagulation disorders [13, 14, 15]. Mice are most commonly used for this purpose [16, 17, 18, 19]. This makes it possible to form large study groups and thus partially compensates for the low reproducibility of these models. Occasionally, rabbits [20] are used for this purpose.

Collagen is often used for the formation of endogenous blood clots either on its own [7, 21] or in combination with epinephrine [14, 17, 22] or norepinephrine [11]. The doses of collagen and epinephrine administered varied within significant limits: dose range for collagen varied from 12.5 µg/kg [23, 24] to 100 mg/kg [25], while for epinephrine it varied from 0.075 µg/kg [24] to 1 mg/kg [26].

Generally, the administered dose of thrombus inducers was determined by calculating the target mortality in the control group. For example, in a study by Crikis et al. [7], isolated intravenous administration of collagen at a dose of 0.075 µg/g was used to model PE in mice. The mortality rate of animals in the control group 1 h after collagen injection was 53%. Ryu et al. [22] induced CTEPH in mice by intravenous administration of collagen (500 µg/kg) in combination with epinephrine (50 µg/kg). Fifteen minutes after drug administration, the mortality was $82.9 \pm 10.7\%$.

Other substances could also be used to induce clot formation in vivo after systemic administration. These include adenosine diphosphate (ADP) [12, 18, 27], thrombin [9, 28, 29], high molecular weight polyphosphate [13], thromboxane A2 receptor agonist U46619 [24], neutrophil elastase [27, 30], arachidonic acid [18], tissue factor [8], or a combination of tissue factor with phospholipids and calcium chloride [13].

Katsumata et al. used ADP as an agent for modeling PE [27]. Here, mice were injected once intravenously with ADP at a dose of 280 mg/kg. The mortality rate in the early stages after introduction of the thrombogenic agent was 43%. It should be noted that isolated use of ADP is rare. The dose of ADP administered varies from 280 mg/kg to 40 mg/100 g [18,27]. An example of such an isolated application of ADP is a study by Katsumata et al. [27], in which mice were injected once intravenously with ADP at a dose of 280 mg/kg. The mortality rate in the early stages after introduction of the thrombogenic agent was 43%.

Hsu et al. [18] used three different prothrombotic agents simultaneously to model PE in mice: ADP, collagen, and arachidonic acid were used at a dose of 40 mg/100 g, 2.5 mg/100 g, and 9 mg/100 g of animal weight, respectively. With intravenous administration of these substances, the death rate from PE was 90% during the first 3 min of observation. The authors indicated differences in the effectiveness of various standard drugs affecting thrombus formation, and the test substance to influence the survival rate of animals after PE. In this study, aspirin and indomethacin have been shown to reduce mortality from PE caused by collagen and arachidonic acid but do not affect survival outcomes using the ADP model. Heparin had no effect on any of the models used. Such differences should be considered when choosing a model to test new drugs that affect thrombus formation.

To increase the efficiency of thrombus formation, a combination of ADP with other prothrombotic agents, such as neutrophil elastase, is occasionally used [27]. Two non-standard approaches to modeling PE were described by Banno et al. [13]. In the first approach, human recombinant tissue factor containing phospholipids and calcium was used as a prothrombotic agent; in the second approach, high molecular weight polyphosphate was used. Polyphosphate is a linear polymer of inorganic phosphates that acts as a natural negatively charged surface that activates the blood coagulation system. Doses of both substances were selected based on 20% survival 20 min after PE in the control group of mice. The authors did not provide comparisons with other available PE models. However, it is likely that the choice of non-standard prothrombotic agents was determined by the aim of the research, which was to study the effect of protein S mutation on venous thromboembolism. Thus, the researchers were primarily interested in the coagulation cascade during thrombus formation, which is facilitated by the agents used in the modeling.

In contrast to the above-described models utilizing non-localized formation of clots in the circulation followed by embolism, there were occasional attempts of PE modeling more closely mimicking the clinical scenario, implying formation of localized thrombi in the limb veins with subsequent displacement and obstruction of pulmonary artery branches. An example of such an approach is a study by Shaya et al. [31], in which the factor V Leiden paradox was investigated; the incidence of deep vein thrombosis was proportionally greater than that of PE in these individuals. To simulate this phenomenon, a piece of filter paper impregnated with 1.8% ferric chloride was applied to the femoral vein. The exposure time was 5 min. After 2 h, the size of the thrombus in situ was assessed, as was the severity of PE.

The above models are characterized by significant variability in the obtained results, which should be considered when planning the sample size. Owing to this, a vast majority of such experiments are performed on readily available mice. Among the advantages, the high pathophysiological accuracy of such models should be pointed out, as this makes it possible to study pharmacological substances with sufficient fidelity to correct the coagulation and aggregation properties of blood.

2.1. Administration of thrombi prepared in vitro

The protocol for modeling PE using thrombotic masses prepared in vitro assumes the initial sampling of animal blood and fabrication of native or modified thrombi of a given size and number, followed by their intravenous administration to the same animal. In some studies, allogeneic [32, 33] or even xenogeneic blood [34, 35, 36] has been used for *in vivo* preparation of thromboemboli. These models are produced in animals of various species, including mice [37, 38, 39], rats [37, 40, 41], hamsters [35, 42, 43], and rabbits [44, 45, 46] (Table 2).

A classic example of PE modeling using *in vitro*-prepared thromboemboli is the modeling protocol used by Tang et al. [47]. In this study, changes in gene expression in the pulmonary artery in the subacute period (7 days) after PE were studied. Rabbits were used, and 0.5 ml of blood was preliminarily collected from the marginal ear vein.

Table 1. PE modelling by blood clots induction *in vivo*.

N ^o	Animal species	Blood clots agents		Aim of study	Administration vessel	Study duration	CTEPH pathway possibility	Authors
		Substance/action	Substance/action					
1	Mice	Collagen + epinephrine	Collagen – 0,8 µg/g; Epinephrine – 60 µg/kg	Studying of catestatin role in blood clots	Inferior vena cava	30 min	–	[100]
2	Mice	Thrombin	20 U	Studying of gelsolin role in PE prevention	Tail vein	15 min	–	[101]
3	Mice	Collagen + epinephrine	Collagen – 400 µg/kg; Epinephrine – 60 µg/kg	Studying of functional role of platelet isoform CD45	retro-orbital sinus	Acute study (After respiratory distress) < 300 s	–	[102]
4	Mice	Collagen + epinephrine	Collagen – 400 µg/kg; Epinephrine – 60 µg/kg	Definition of functional role of ELMO1 peptide in platelets	Intravenous (n/d)	Acute study (After respiratory distress)	–	[103]
5	Mice	Application of ferric chloride (III)-(soaked filter paper) on femoral vein	Size of filter paper - 1 x 2 mm. FeCl ₃ concentration– 1,8%. Exposure time – 5 min	Studying of generation rate, stability and embolization risk in case of factor V Leiden (FVL) variant	Femoral vein	2 h	–	[31]
6	Mice	Collagen + epinephrine	Collagen – 280 µg/kg; Epinephrine – 29 µg/kg	Studying of inhibitor tyrosineprotein kinase MER effectiveness in platelets inactivation and blood clots prevention	Intravenous (n/d)	15 min	–	[104]
7	Mice	1) Thromboplastin 2) Collagen + epinephrine	Thromboplastin – 5 µL; Collagen – 64 µg/kg; Epinephrine – 5,4 µg/kg	Studying of platelets TLT-1 receptor role of immune origin hemorrhage	Intravenous (n/d)	30 min	–	[105]
8	Mice	Collagen/2MeSADP + epinephrine	Collagen – 400 µg/kg; 2MeSADP – 20 µg/kg; Epinephrine – 30 µg/kg	Studying of platelets activation mechanisms in case of hemostasis	retro-orbital sinus/ Inferior vena cava	Acute study (After respiratory distress)	–	[106]
9	Mice	Collagen + epinephrine	Collagen – 430 µg/kg; Epinephrine – 20 µg/kg	Studying of glucose metabolism effect on platelets function regulation	Intravenous (n/d)	25 min	–	[14]
10	Mice	Collagen + epinephrine	Collagen – 500 µg/kg; Epinephrine – 50 µg/kg	Studying of thrombin inhibitor anticoagulant potency in PE prevention	Tail vein	15 min	–	[107]
11	Mice	Thromboplastin	7,5 µL/g	Studying of the vaccination anticoagulant properties to factor XI in thrombosis prevention	Intravenous (n/d)	3 min	–	[8]
12	Mice	Collagen + epinephrine	Collagen – 0,6 µg/g; Epinephrine – 0,2 µg/g	Study of the thromboxane receptor antagonist antiplatelet properties in PE prevention	Tail vein	Acute study (After respiratory and heartbeat distress)	–	[17]
13	Mice	Collagen + epinephrine	Collagen – 500 µg/kg; Epinephrine – 50 µg/kg	Studying of the antithrombotic and anticoagulant activity of alkaloids Scolopendra subspinipes mutilans	Tail vein	15 min	–	[108]
14	Mice	1) Tissue factor (human recombinant) with phospholipids and calcium 2) High molecular polyphosphate	Till 80% mortality after 20 min after administration	Assessment of protein S mutation role in the development of venous blood clots in PROS1 knockout mice	Inferior vena cava	20 min	–	[13]
15	Mice	Collagen + epinephrine	Collagen – 0,5 µg/kg; Epinephrine – 0,06 µg/kg	Studying of the limiglydol antiplatelet properties in PE prevention	Tail vein	1 day	–	[109]

(continued on next page)

Table 1 (continued)

№	Animal species	Blood clots agents		Aim of study	Administration vessel	Study duration	CTEPH pathway possibility	Authors
		Substance/action	Substance/action					
16	Mice	Splenectomy followed after 1 month narrowing of the inferior vena cava lumen, by ligation	–	Studying of splenectomy role in CTEPH formation	–	1–28 days	CTEPH +/- (after 28 days pressure in PA wasn't measured)	[92]
17	Mice	Thrombin	1500 IU/kg body weight	Studying of the antithrombotic properties of N-acylhydrazone	Tail vein	15 min	–	[28]
18	Mice	Collagen + epinephrine/collagen + epinephrine + amyloid β	Collagen – 1000 $\mu\text{g}/\text{kg}$; Epinephrine – 10 $\mu\text{g}/\text{kg}$; Amyloid β – 2,5 mg/kg	Studying of amyloid β role in thrombosis	Tail vein	15 min	–	[15]
19	Mice	Thrombin	1250 IU/kg body weight	Evaluation of the nanocarrier effectiveness for enhancing oral delivery of enoxaparin	Tail vein	15 min	–	[9]
20	Mice	1. Collagen + norepinephrine 2. Thrombin	1. Collagen – 500 $\mu\text{g}/\text{kg}$; norepinephrine – 80 $\mu\text{g}/\text{kg}$. 2. Thrombin - 2000 IU	Studying of the antithrombotic properties of N-acylhydrazone	Intravenous (n/d)	15 min	–	[11]
21	Mice	Thromboplastin	1–1,33 mg/mice	Testing of thrombosis diagnostic systems	Tail vein	30 min	–	[110]
22	Mice	Collagen	Collagen – 0,4 mg/kg	Studying of the anopheline antiplatelet properties in the PE prevention	Tail vein	1 h	–	[21]
23	Mice	Collagen + epinephrine	Collagen – 80 mg/kg ; Epinephrine – 1 mg/kg	Research on the antiplatelet properties of argan oil	Tail vein	15 min	–	[26]
24	Mice	Collagen	0,075 $\mu\text{g}/\text{g}$ body weight	Study of the thrombomodulin anticoagulant effect	external jugular vein	1 h	–	[7]
25	Mice	Collagen + epinephrine	Collagen – 500 $\mu\text{g}/\text{kg}$; Epinephrine – 50 $\mu\text{g}/\text{kg}$	Evaluation of the antithrombotic properties of Ginkgo biloba and cilostazol combination	Tail vein	15 min	–	[22]
26	Mice	Neutrophil elastase + collagen-induced arthritis	Neutrophil elastase – 5 U/kg. 2 times per day administration during 3 days	Studying of the neutrophilic elastase role in the PE development. Evaluation of the recombinant soluble thrombomodulin effects in reducing the PE risks.	Tail vein	4 days after last injection	–	[30]
27	Mice	Collagen + epinephrine/U46619	Collagen – 12,5 $\mu\text{g}/\text{kg}$; Epinephrine – 0,075 $\mu\text{g}/\text{kg}$; U46619 – 0,2 mg/kg	Study of the NO-releasing statin antithrombotic properties of	Intravenous (n/d)	15 min	–	[23]
28	Mice	Thromboplastin	Thromboplastin – 65 $\mu\text{L}/\text{kg}$ or 140 $\mu\text{L}/\text{kg}$	Studying of CD39 antiplatelet properties on liposomes in the PE prevention	Jugular vein	30 min	–	[111]
29	Mice	Collagen III type + epinephrine	Collagen – 100 mg/kg ; Epinephrine – 90 $\mu\text{g}/\text{kg}$	Investigation of the type III collagen derivatives antithrombotic properties	Jugular vein	8 min	–	[25]
30	Mice	Collagen + epinephrine	Collagen – 800 $\mu\text{g}/\text{kg}$; Epinephrine – 60 $\mu\text{g}/\text{kg}$	Studying of the $\alpha_2\text{A}$ -adrenergic receptors role in platelet activation	Jugular vein	5 min	–	[112]
31	Mice	ADP/NE + ADP	NE – 10 $\mu\text{g}/\text{mouse}$; A_2A – 28 $\text{mg}/100 \text{ g}$	Studying of the neutrophilic elastase role in the PE development	Intravenous (n/d)	Acute experiment (n/d)	–	[27]

(continued on next page)

Table 1 (continued)

N ^o	Animal species	Blood clots agents		Aim of study	Administration vessel	Study duration	CTEPH pathway possibility	Authors
		Substance/action	Substance/action					
32	Mice	Collagen + epinephrine	Collagen – 12,5 µg/mouse Epinephrine – 0,075 µg/mouse	Investigation of the combination of nitroaspirin and clopidogrel antiplatelet properties in the PE prevention	Intravenous (n/d)	2 min	–	[113]
33	Mice	Collagen + epinephrine/U46619 — agonist to A ₂ thromboxane receptors	Collagen - 12,5 µg/kg; Epinephrine – 0,075 µg/kg U46619 – 0,2 µg/kg	Studying of the NO-releasing statin antithrombotic properties	Intravenous (n/d)	15 min	–	[24]
34	Mice	Collagen + epinephrine/collagen	Collagen – 25/12/6/3 µg; Epinephrine – 1 µg	Studying of the α2β1 integrin role in the platelet aggregation and thrombus formation	Right Jugular vein	3 min	–	[19]
35	Mice	Thrombin	It was counted as a 90% mortality dose	Studying of low molecular weight heparins anticoagulant action mechanisms	Tail vein	15 min	–	[114]
36	Mice	Thrombin	1250 IU/kg body weight	Investigation of the protein C anticoagulant properties in blood clots prevention	Tail vein	15 min	–	[29]
37	Mice	Collagen + epinephrine	collagen – 400 µg/kg; epinephrine – 50 µg/kg	Study of the glycoprotein IIb/IIIa antagonist antiplatelet properties in the PE prevention	Tail vein	15 min	–	[16]
38	Mice	ADP	300 µg/g body weight	Assessment of the drug antithrombotic properties	Tail vein	10 min	–	[12]
39	Mice	Collagen + epinephrine	collagen – 25 µg; epinephrine – 1,5 µg	Evaluation of the antithrombotic drugs effectiveness in the PE prevention	Tail vein	3 min	–	[10]
40	Mice and rabbits	Mice: human thrombin/collagen + epinephrine; Rabbits: thrombin/ADP/platelets activating factor	Mice: human thrombin 1250 IU/kg, collagen 1,25 mg/kg, epinephrine 75 µg/kg Rabbits: thrombin 10/20 IU/kg or ADP 20 µg/kg or platelets activating factor – 50 ng/kg.	Studying of the anticoagulant and antiplatelet properties of defibrinolytic	Mice – tail vein; Rabbits – marginal auricular vein	Mice – 15 min; Rabbits – 5 min	–	[20]
41	Mice	Thrombin	Thrombin (0, 25, 50, 75 IU/mouse)	Studying of the thrombomodulin anticoagulant properties in the PE prevention	Tail vein	15 min	–	[115]
42	Mice	Thrombin	3,8–15 IU/mouse	Studying of the thrombomodulin role in the PE pathogenesis	Tail vein	1 h	–	[116]
43	Mice	ADP/collagen/arachidonate	ADP – 400 mg/kg; Collagen – 25 mg/kg; Arachidonate – 90 mg/kg	Studying of the Agrimonia pilosa extract antiplatelet properties in the PE prevention	Intravenous (n/d)	3 min	–	[18]

Note: ADP — adenosinediphosphate, i/v — intravenous administration, IU — international unit, PE — pulmonary embolism, CTEPH — chronic thromboembolic pulmonary hypertension, 2MeSADP — 2-methylthio-adenosine-5'-diphosphate, n/d — no data, NO — nitrogen oxide (II), NE — neutrophil elastase, U46619 — 9,11-dideoxy-11a,9a-epoxymethanoprostaglandin F2a.

Subsequently, thrombotic masses were formed under sterile conditions at room temperature for 45 min, from which embolizing particles 5-mm long were prepared by cutting. Blood clots were suspended in 10 ml of normal saline and injected into the femoral vein. An additional 5 ml of saline was used to flush the catheter and advance the thromboemboli.

In the majority of studies, tubes of corresponding diameter were used for the formation of thromboemboli of given sizes. A thrombotic mass

formed inside each tube, and the resulting thrombotic mass was cut to the desired length, giving it the characteristics of the desired naturally occurring thromboembolus [48, 49].

To accelerate the formation of thrombotic masses in vitro in a number of studies, thrombin [33, 50, 51], tissue factor [49], and calcium chloride [50, 51, 52] were used. As mentioned above, rodent blood has a high fibrinolytic activity, which leads to rapid lysis of exogenously administered blood clots. In order to overcome this problem, fibrinolysis

Table 2. Administration of thrombi prepared *in vitro*.

№	Animal species	Embolizing particles					Preparation conditions	Aim of work	Vessel of sampling/administration	Study duration	Possibility of CTEPH formation	Authors
		Material	Label	Size	Dose							
1	Mice	Autologous thrombi	–	1 × 1 mm	30 pcs	–	Studying of miR-106b-5p role in PE	Blood sampling – tail vein	7 days	–	[117]	
2	Mice	Xenogenic fibrinous thrombi (human plasma)	¹²⁵ I-labeled fibrin	12,5 μL	20 pcs	<i>in vitro</i> addition of CaCl ₂ and thrombin	Study of α2-antiplasmin contribution to fibrinolytic insufficiency	TE administration – jugular vein	4 h	–	[39]	
3	Mice	Autologous fibrinous thrombi	–	1 × 1,2 mm	30 pcs	<i>in vitro</i> addition of CaCl ₂ and thrombin	Study of mesenchymal stem cells use effectiveness in acute PE	Blood sampling – tail vein; TE administration – jugular vein	1 day	–	[118]	
4	Mice	Xenogenic fibrinous thrombi (human plasma)	¹²⁵ I-labeled fibrin	1,5–5 μm	–	<i>in vitro</i> addition of CaCl ₂ and thrombin	Study of t-PA, tenecteplase and reteplase fibrinolytic capacity in PE	TE administration – jugular vein	1 h	–	[119]	
5	Mice	Fibrinous thrombi	¹²⁵ I-labeled fibrin	–	–	–	Study of pulmonary vascular activity regulation using tissue plasminogen activator via NMDA receptors	TE administration – jugular vein	1 h	–	[120]	
6	Mice	Autologous fibrinous thrombi	–	1,2 × 1 mm	30 TE	<i>in vitro</i> addition of CaCl ₂ and thrombin	Study of the number and function of endothelial precursors from the bone marrow in acute PE in mice.	Blood sampling – tail vein. TE administration – jugular vein	1 h, 1 day, 2 days	–	[51]	
7	Mice	Autologous fibrinous thrombi	¹²⁵ I-labeled fibrin	–	25 μL	–	Study of fibrinolytic properties during adenoviral transfection of the plasminogen activator gene in mice with varying degrees of tPA deficiency	TE administration – jugular vein	16 h	–	[38]	
8	Mice	Xenogenic thrombi from modified RBC (rats RBC)	–	–	–	Chlorpromazine and glutaraldehyde were added	New model development	Blood sampling – blood rats; TE administration – tail vein	15 min	–	[36]	
9	Mice и rats	Fibrinous thrombi	¹²⁵ I-labeled fibrin	3–5 μm	–	<i>in vitro</i> addition of CaCl ₂ and thrombin	Study of the tPA fibrinolytic activity associated with RBC in the thrombosis prevention	–	1 h	–	[37]	
10	Rats	Autologous thrombi + tranexamic acid + carrageenan	–	–	32 ± 5	Administration was repeated after 4 and 11 days from the 1st administration	Study of the aseptic inflammation role in the CTEPH formation	Blood sampling – external jugular vein. TE administration – jugular vein	32 days	CTEPH +	[90]	

(continued on next page)

Table 2 (continued)

№	Animal species	Embolizing particles					Preparation conditions	Aim of work	Vessel of sampling/administration	Study duration	Possibility of CTEPH formation	Authors
		Material	Label	Size	Dose							
11	Rats	Autologous thrombi	–	1 × 2 mm	30 TE	–	Urokinase effect on PE formation	Blood sampling – tail vein. TE administration – jugular vein	6 h	–	[121]	
12	Rats	Autologous thrombi + tranexamic acid	–	1 × 3 mm	Administration was repeated after 4 and 7 days from the 1st administration	–	Study of transcription factor O-1 and apoptosis role in remodeling of pulmonary artery branches in CTEPH	Blood sampling – orbital vein. TE administration – jugular vein	1, 2 and 4 weeks	CTEPH +	[86]	
13	Rats	Autologous thrombi	–	1,1 × 2 mm	25 TE	Incubation on water bath 70 °C, 10 min	Evaluation of low molecular weight heparin effect on intimal hyperplasia in acute PE.	Blood sampling – tail vein. TE administration – jugular vein	1, 4, 7, 14 and 28 days	CTEPH +	[85]	
14	Rats	Autologous thrombi + tranexamic acid	–	1 × 3 mm	40 TE; Administration was made 2 times with 4 days interval	–	Study of the tissue factor and transcription factor O-1 expression in CTEPH modelling	Blood sampling – orbital vein. TE administration – jugular vein	1, 2 and 4 weeks	CTEPH +	[53]	
15	Rats	Autologous thrombi + tranexamic acid	–	1 × 3 mm	Administration was made 2 times with 4 days interval	–	Study of the tissue factor and autophagy role in the remodeling of pulmonary artery branches in CTEPH	Blood sampling – orbital vein. TE administration – jugular vein	1, 2 and 4 weeks	CTEPH +	[87]	
16	Rats	Autologous thrombi + tranexamic acid	–	3 mm × 1 mm	15 emboli. Administration was made 3 times with 2 weeks interval	0.2 ml of blood, 37 °C till night	Study of the ginsenoside substance Rg1 effect on fibrous myocardial remodeling in CTEPH	Blood sampling – tail vein; TE administration – jugular vein	4 weeks – preparation time; + 4 weeks of observing	CTEPH +	[88]	
17	Rats	Autologous thrombi	–	~2 mm ³	15-20 pcs	–	Study of the aspirin effects on ERK and PI3K/Akt signaling pathways in PE	Blood sampling – orbital vein; TE administration – jugular vein	3 days	–	[41]	
18	Rats	Autologous thrombi	–	1,1 × 3 mm	0,5 mL (18 mg/100 g)	<i>in vitro</i> addition of CaCl ₂ and thrombin	Chimeric antibodies to MCP-1 suppress the development of acute pulmonary hypertension after PE	Blood sampling – carotid; TE administration – jugular vein	1, 4 and 8 h	–	[52]	
19	Rats	Allogenic fibrinous thrombi	¹²⁵ I-labeled fibrin	10–100 μm	75 μL/kg	<i>in vitro</i> addition of CaCl ₂ and thrombin	Study of the SMTP substance fibrinolytic properties after PE	TE administration – tail vein	20 min	–	[40]	
20	Two rats lines: Sprague-Dawley и Copenhagen	Autologous thrombi + tranexamic acid	–	SD – 1,4 mm diameter; Cop. – 1,14 mm diameter	SD – 18 mg/100 g; Cop. – 5 mg/100 g	<i>in vitro</i> addition of CaCl ₂ and thrombin	PE modelling with fibrinolysis suppression and stimulation of coagulation on different rats' species	Blood sampling – jugular vein. TE administration – jugular vein	1 and 5 days	–	[50]	

(continued on next page)

Table 2 (continued)

№	Animal species	Embolizing particles					Preparation conditions	Aim of work	Vessel of sampling/ administration	Study duration	Possibility of CTEPH formation	Authors
		Material	Label	Size	Dose							
21	Rats	Allogenic thrombi	–	10 mm × 1,5 mm	3 TE	<i>in vitro</i> addition of thrombin	Study of plasma proteome changes in acute PE	TE administration - jugular vein	1, 8, 24, 48 h	–	[48]	
22	Rats	Allogenic thrombi	–	10 × 1,5 mm	3 TE	<i>in vitro</i> addition of thrombin	Study of paracrine factors in acute PE	Blood sampling – from another rats (cardiac puncture). TE administration – jugular vein	1, 8, 24 and 48 h	–	[33]	
23	Rats	Xenogenic fibrinous thrombi (rabbit plasma)	–	–	–	–	Study of targeted thrombolysis of monoclonal antibodies chimeric molecules to the pulmonary artery endothelium and urokinase.	TE administration – jugular vein	2 h	–	[34]	
24	Rats	Allogenic fibrinous thrombi	¹²⁵ I-labeled fibrin	10–100 μm	–	<i>in vitro</i> addition of CaCl ₂ and thrombin. Thrombi were frozen by liquid nitrogen before blending	Study of the surfactin C effect on the fibrinolytic capacity of plasma caused by the plasminogen activation in PE	TE administration – tail vein	80 min	–	[122]	
25	Rats	Allogenic thrombi	–	–	–	–	Study of RV and LV dysfunction in massive acute PE	Blood sampling – donor femoral artery. TE administration – jugular vein	30 min	–	[32]	
26	Rats	Allogenic thrombi	¹²⁵ I-labeled fibrin	1,47 × 12 mm	1 TE	<i>in vitro</i> addition of CaCl ₂ and thromboplastin	Study of thrombolytic properties of Desmodus Rotundus salivary plasminogen activator in PE	Blood sampling – carotid (rat-donor); TE administration - jugular vein	1 h	–	[49]	
27	Rats and hamsters	Rat – allogenic fibrinous thrombi; hamsters – xenogenic fibrinous thrombi (human plasma)	¹²⁵ I-labeled fibrin	–	–	–	2 models comparison. Evaluation of t-PA effect	TE administration – inferior vena cava	2,5 h	–	[123]	
28	Hamsters	Xenogenic fibrinous thrombi (human plasma)	¹²⁵ I-labeled fibrin	–	50 μL	–	Study of thrombolytic and antiplatelet properties of a recombinant chimeric molecule containing an activated platelet agonist and single-chain urokinase.	TE administration – jugular vein	1,5 h	–	[35]	

(continued on next page)

Table 2 (continued)

N ^o	Animal species	Embolizing particles					Aim of work	Vessel of sampling/ administration	Study duration	Possibility of CTEPH formation	Authors
		Material	Label	Size	Dose	Preparation conditions					
29	Hamsters	Xenogenic fibrinous thrombi (human plasma)	¹²⁵ I-labeled fibrin	–	25 µL	–	Study of the recombinant t-PA anticoagulant activity with a Lys296-Gly302 deletion	TE administration – left jugular vein	1,5 h	–	[54]
30	Hamsters	Xenogenic fibrinous thrombi (human plasma)	¹²⁵ I-labeled fibrin	–	25 µL	–	Study of thrombolytic and antiplatelet properties of a conjugated molecule consisting of u-PA and monoclonal antibodies to platelets	TE administration – jugular vein	1,5 h	–	[43]
31	Hamsters	Autologous fibrinous thrombi	¹²⁵ I-labeled fibrin	–	25 µL	–	Comparative study of bolus thrombolytic properties and continuous administration of a chimeric plasminogen activator molecule (t-PA/u-PA)	TE administration – jugular vein	1,5 h	–	[42]
32	Rabbits	Autologous thrombi	–	3 × 10 mm	Mean number of thrombi 4,9 ± 1,2 (before shocked)	–	Study of sodium nitroprusside and diltiazem effect on the sympathetic nervous system activation.	Blood sampling – femoral vein. TE administration – pulmonary artery (catheterized through the femoral vein)	2 h	–	[96]
33	Rabbits	Autologous thrombi	–	3 × 10 mm	Mean number of thrombi 4,9 ± 1,2 (before shocked)	–	Study of the sodium nitroprusside effects on hemodynamics in massive PE with cardiogenic shock	Blood sampling – femoral vein. TE administration – pulmonary artery (a catheter passed through the femoral vein)	2 h	–	[57]
34	Rabbits	Autologous thrombi	–	1 × 3–4 mm	Thrombi from 1 ml of blood	Incubation on water bath 70 °C, 10 min	Study of the nitric oxide inhalation effect on troponin I and blood clotting factors during massive PE	Blood sampling – auricular vein. TE administration – jugular vein	120 min	–	[46]
35	Rabbits	Autologous thrombi	–	1–2 mm	Thrombi from 1 ml of blood	–	Assessment of hemodynamic changes during acute PE	Blood sampling – jugular vein. TE administration – jugular vein	<1 h	–	[56]
36	Rabbits	Autologous thrombi	–	0,8–1 mm	Thrombi from 1 ml of blood	–	Assessment of hemodynamic changes during acute PE	Blood sampling – jugular vein. TE administration – jugular vein	5 min	–	[55]

(continued on next page)

Table 2 (continued)

№	Animal species	Embolizing particles					Aim of work	Vessel of sampling/administration	Study duration	Possibility of CTEPH formation	Authors
		Material	Label	Size	Dose	Preparation conditions					
37	Rabbits	Autologous thrombi	–	5 mm	Thrombi from 0,5 ml of blood	–	Study of gene expression changes in the pulmonary artery during the subacute period (7 days) after PE	Blood sampling – marginal auricular vein. TE administration – jugular vein	7 days	–	[47]
38	Rabbits	Autologous thrombi	–	2–4 mm diameter, 7–10 mm length	2 pcs	<i>in vitro</i> addition of thrombin	Changes in tissue factor expression in rabbits during acute PE	Blood sampling – marginal auricular vein. TE administration – jugular vein	3, 8 and 24 h	–	[44]
39	Rabbits	Autologous thrombi	–	2 × 20 mm	–	–	Study of FIIa enzyme fibrinolytic activity from the Agkistrodon acutus venom in acute PE	TE administration – through a catheter in the RV	2 h	–	[45]
40	Rabbits	Autologous thrombi	–	–	Thrombi from 10 ml or 1 ml of blood	–	Comparison of the traditional iodine-containing contrast effectiveness and contrast agent based on the liposomal pool of blood in PE	Blood sampling – auricular vein. TE administration – ental jugular vein	270 min	–	[58]

Note: RV — right ventricular, TE — thromboemboli, PE — pulmonary embolism, CTEPH — chronic thromboembolic pulmonary hypertension, CaCl₂ — calcium chloride, ¹²⁵I — iodine-125 labelled, MCP-1 — monocyte attractant protein - 1, SD — Sprague-Dawley, Cop. — Copenhagen, t-PA — tissue plasminogen activator, u-PA — urokinase plasminogen activator.

inhibitors such as tranexamic acid have been used to suppress the fibrinolytic activity [50, 53].

The activity of the fibrinolytic system may vary depending on the genetic background of animals of the same species. For instance, Copenhagen rats were found to have lower fibrinolytic activity than Sprague-Dawley (SD) rats [50]. An intravenous administration of *ex vivo* formed thromboemboli with tranexamic acid caused a concomitant inhibition of fibrinolysis, resulting in a significant increase in systolic pressure in the right ventricle (RV) (45–55 mmHg) immediately after the intravenous administration of the thromboemboli, followed by normalization of the systolic pressure in the RV within 24 h in SD rats and within 5 days in Copenhagen rats. Lysis of thromboemboli after 24 h and 5 days was 95% and 97% in SD rats, and 70% and 87% in Copenhagen rats, respectively. Thus, even in Copenhagen rats, the degree of thromboemboli lysis was high enough to sustain elevated pressure in the RV for more than 5 days, which leads to the conclusion that such an approach is inappropriate for modeling persistently increased pressure in the RV and in the development of CTEPH.

Although whole blood is most commonly used to form thromboemboli *ex vivo*, in some cases, only certain components are used, for example, blood plasma from which fibrin clots are formed. Fibrin clots are more suitable for preclinical studies on the effectiveness of new fibrinolytic modifications [38, 42]. Moreover, such thromboemboli can be better standardized in size and provided with isotope labeling, as shown by Murciano et al. [37].

In addition to the introduction of the label, other modifications of thromboemboli can be used to achieve the required properties. For example, to study new approaches to the treatment of PE, which are not

associated with an effect on platelets, a model was proposed to modify erythrocytes with chlorpromazine, which has antihemolytic properties, and glutaraldehyde, which causes fixation of erythrocytes [36]. This modification made red blood cells more resistant to lysis.

In mice, rats, and hamsters, this type of model is most often used to test new thrombolytic [35, 37, 38] and anticoagulant [54] substances. A number of studies on changes in the level of paracrine factors in PE have been carried out to reveal the genetic basis of pathological processes that occur in the acute and subsequent periods of PE [33, 48, 53].

In rabbit models, changes in gene expression in the pulmonary artery and lung tissue were studied at different periods after PE [44, 47], changes in hemodynamics during acute PE were assessed [55, 56], drugs were tested for the correction of hemodynamic disorders [46, 57] and new contrast agents were tested for computed tomography [58].

This type of model is characterized by a significantly greater standardization than PE models reproduced by the formation of endogenous thrombi. The use of radioactive labels such as ¹²⁵I-labeled fibrin allows a detailed assessment of the distribution of blood clots in the bloodstream and their fate [35, 37, 38, 42]. Among the disadvantages of these models, it is worth noting the technical complexity and need for repetitive surgical interventions while using autologous blood clots.

2.2. Administration of non-thrombotic particles

Modeling of PE with non-thrombotic particles, consisting of natural or synthetic polymers, is most often performed in rats and rabbits, while the approaches to modeling and goals differ greatly between these species (Table 3).

Table 3. Administration of particles non-thrombotic nature.

№	Animal species	Embolizing particles			Aim of work	Administration vessel	Study duration	CTEPH pathway possibility	Authors
		Material	Size	Dose					
1	Rats	Sodium alginate microspheres	180 ± 28 µm	9367 ± 551 per animal	CTEPH modelling	Tail vein	8 times at 4-day intervals	CTEPH +	[93]
2	Rats	Polystyrene microspheres	26 µm	0,75 ml/kg	Studying of the RAS role in PE severity	Jugular vein	5 h	–	[124]
3	Rats	Microspheres Sephadex G50	300 µm	12 mg/kg	Role of cyclophilin A-CD147 in RV injury and dysfunction after PE	Right femoral vein	6, 12, 24, 48, and 72 h	–	[125]
4	Rats	Polystyrene microspheres	25 ± 1 µm	1,3 × 10 ⁶ /100 g of body weight	Studying of HIF-1α expression and its correlation with pulmonary artery and RV remodeling in PE	Right jugular vein	12 weeks	CTEPH +	[60]
5	Rats	Polystyrene microspheres + inhibitor of tyrosinekinase receptor VEGF (SU5416)	85 µm	97 × 10 ³ /100 g of body weight	CTEPH modelling	Tail vein	3 weeks/6 weeks	CTEPH +	[91]
6	Rats	Polystyrene microspheres collagen-fibrin coated, suspended in thrombin solution	45 µm	3 administrations were done: 1 × 10 ³ /1 g of body weight (1st, 2nd administrations), 0,75 × 10 ³ /1 g of body weight (3rd administration)	CTEPH modelling	Tail vein	9 days after last administration	CTEPH +/- (short observation time)	[61]
7	Rats	Polystyrene microspheres	25 ± 1 µm	1,95 × 10 ⁶ /100 g of body weight; Administration was done during 10 min	Studying of the stimulant soluble guanylate cyclase effect on RV after pulmonary embolism	Right jugular vein	5 hours/18 h	–	[63]
8	Rats	Polystyrene microspheres	25 µm	1,8 × 10 ⁶ /100 g of body weight	Studying of PE pathogenesis	Right jugular vein	18 h	–	[126]
9	Rats	Polystyrene microspheres	25 µm	1,8 × 10 ⁶ /100 g of body weight	Studying of the increased expression of type 2 arginase role on vasoconstriction in pulmonary embolism	Right jugular vein	18 h	–	[65]
10	Rats	Polystyrene microspheres	25 µm	1,3 or 1,6 × 10 ⁶ /100 g of body weight	Investigation of the soluble guanylate cyclase stimulator effect in pulmonary embolism	Right jugular vein	5 h	–	[127]
11	Rats	Polystyrene microspheres	26 µm	1,5 mL/kg	Studying of the Rho-kinase role in PE pathogenesis	RV	6 h	–	[128]
12	Rats	Polystyrene microspheres	25 ± 1 µm	1,3 or 1,65 or 2,0 × 10 ⁶ /100 g of body weight	Studying of the plasma proteins relation with the development of pulmonary hypertension after pulmonary embolism	Jugular vein	18 h	–	[66]

(continued on next page)

Table 3 (continued)

N ^o	Animal species	Embolizing particles			Aim of work	Administration vessel	Study duration	CTEPH pathway possibility	Authors
		Material	Size	Dose					
13	Rats	Polystyrene microspheres	24 ± 1 μm	2,0 × 10 ⁶ /100 g of body weight	Investigation of inflammation in case of RV injury in PE	Right jugular vein	1 day–6 weeks	–	[62]
14	Rats	Microparticles Sephadex G50	300 μm	–	Investigation of atorvastatin effects in PE	Tail vein	24 h	–	[72]
15	Rats	Polystyrene microspheres	25 ± 1 μm	2,08 × 10 ⁶ /100 g of body weight	Investigation of inflammation in case of RV injury in PE	Right jugular vein	20 h	–	[64]
16	Rats	Microparticles Sephadex G50	300 μm	9 mg/kg	Investigation of doxycycline hemodynamic effects in PE	Left femoral vein	1 h	–	[71]
17	Rats	Polystyrene microspheres	24 ± 1 μm	0,05 ml/100 g of body weight	Studying of the thromboxane synthase and cyclooxygenase inhibition effects in pulmonary embolism	Left jugular vein	17 h	–	[129]
18	Rats	Polystyrene microspheres	24 ± 1 μm	1,3/1,95 (× 10 ¹⁰ /kg)	Studying of pulmonary embolism and following pulmonary hypertension binding, associated with the development of aseptic inflammation	Jugular vein	18 h	–	[59]
19	Rats	Latex microspheres	24 ± 1 μm	0,125 ml per 100 g of body weight Repeated administrations were done with 1 min interval till aimed pressure in pulmonary artery	Studying of the massive PE effects on the concentration of carbon dioxide during expiration	Left jugular vein	40–45 min	–	[68]
20	Rats	Latex microspheres	25,7 ± 5,8 μm	–	Development of PE model with a controlled increase in pulmonary artery pressure	Pulmonary artery	24 h	–	[67]
21	Rats	Carbon fiber composite microspheres	15 ± 5 μm	0,013/0,01 g per 100 g of body weight	Studying of myocardium ultrastructural changes in the early stages after PE	Subcutaneous vein	1 h/24 h for doses 0,013/0,01 g per 100 g of body weight, respectively	–	[69]
22	Rabbits	Graphite microspheres	5 μm	1 cubic centimeter (cc.) per pound of body weight	Studying of the sympathetic nervous system role in vasospasm in the acute period of pulmonary embolism	–	15 min	–	[70]
23	Rabbits	Gelatine sponge	4 × 4 × 10 mm or 2 × 4 × 10 mm	4 pcs	Dual-energy computed tomography testing for pulmonary embolism	Femoral vein	7 days	–	[76]

(continued on next page)

Table 3 (continued)

N ^o	Animal species	Embolizing particles			Aim of work	Administration vessel	Study duration	CTEPH pathway possibility	Authors
		Material	Size	Dose					
24	Rabbits	Gelatine sponge	4 × 4 × 10 mm / 2 × 4 × 10 mm	4 pcs	Dual-energy computed tomography testing for pulmonary embolism	Right femoral vein	2 h	–	[79]
25	Rabbits	Gelatine sponge	4 × 4 × 10 mm / 2 × 4 × 10 mm	4 pcs	Dual-energy computed tomography testing for pulmonary embolism	Right femoral vein	2 h	–	[78]
26	Rabbits	Intravascular silicone balloon in left/right pulmonary artery	–	–	Comparison of the time-resolved MRI and high-resolution MRI angiography effectiveness for the PE detection	Femoral vein	Acute experiment	–	[74]
27	Rabbits	Gelatine sponge	4 × 2 × 10 mm / 2 × 2 × 10 mm	4 pcs	Dual-energy computed tomography testing for pulmonary embolism	Right femoral vein	2 h	–	[77]
28	Rabbits	Intravascular silicone balloon in left pulmonary artery	–	–	Testing of contrast agents for MRI diagnostics of pulmonary embolism	Right femoral vein	Acute experiment	–	[75]
29	Rabbits	Gelatine sponge	4 × 4 × 10 mm / 2 × 4 × 10 mm	4 pcs	Dual-energy computed tomography testing for pulmonary embolism	Right femoral vein	2 h	–	[80]
30	Rabbits	Intravascular silicone balloon in left pulmonary artery	–	–	Testing of contrast agents for ventilation-perfusion MRI diagnostics of pulmonary embolism	Femoral vein	Acute experiment	–	[73]

Note: MRI — magnetic resonance imaging, RV — right ventricular, RAS — renin-angiotensin system, PE — pulmonary embolism, CTEPH — chronic thromboembolic pulmonary hypertension, HIF-1 α — factor induced by hypoxia - 1 α , VEGF — vessel endothelial growth factor.

In rats, polystyrene microspheres are most often used as embolizing particles [59, 60, 61, 62]. The standard diameter of microparticles is 23–26 μm [59, 63, 64]. For example, Watts et al. [65] used polystyrene microspheres with a diameter of 25 μm in the form of a 10% suspension (1.3×10^6 microspheres/ml). Microspheres were injected into the right jugular vein at a dose of 1.8×10^6 per 100 g in anesthetized male SD rats weighing 350–400 g. According to the data of wire myography, 18 h after embolization, a significant decrease in relaxation of the vascular rings of the pulmonary artery in response to acetylcholine exposure was observed in experimental animals compared to controls.

A similar protocol was used by Zagorski et al. [66], where male SD rats weighing 375–450 g were injected with a suspension of polystyrene microspheres $25 \pm 1 \mu\text{m}$ in 0.01% Tween-20 to a final concentration of 13×10^6 microspheres per ml. Three different doses of microspheres ($1.3 \times 10^6/100$ g, $1.65 \times 10^6/100$ g, and $2.0 \times 10^6/100$ g) were injected into the jugular vein of an anesthetized animal. The study showed a dose-dependent increase in systolic pressure in the RV at 2 h and 18 h post-embolization.

In addition to polystyrene microspheres, latex [67, 68], carbon fiber [69] graphite [70] and Sephadex [71, 72] microparticles have also been used in rats.

In a study by Riegger et al. [67], latex microparticles were used to model PE in rats. Anesthetized male Wistar rats weighing 300–350 g were injected with latex microspheres of $25.7 \pm 5.8 \mu\text{m}$ in diameter through a catheter placed in the pulmonary artery until a mean pulmonary artery pressure of 35 mmHg was reached.

In a number of studies, Sephadex microspheres (Pharmacia Biotech, Germany) were used. They are gel filtration resins obtained by cross-linking dextran with epichlorohydrin [71, 72]. Palei et al. [71] performed experiments on male Wistar rats (240–280 g) by injecting them with Sephadex G50 microspheres at a dose of 9 mg/kg and an embolizing particle size of 300 μm , to simulate PE. The authors indicated in pilot studies that various doses of microspheres were tested in the range of 5–15 mg/kg. The 9 mg/kg dose was chosen because it induced a significant systemic arterial hypotension but did not lead to death. Sixty minutes after embolization, the mean arterial pressure decreased by 25.5 ± 4.4 mmHg.

Models based on the use of non-thrombotic emboli are also used in rabbits. However, the materials used to fabricate emboli in rabbits differ significantly from those used in rats. This difference is in part due to the larger size of the pulmonary artery in rabbits, thus allowing the intravascular delivery and positioning of emboli. For example, intravascular delivery of a silicone balloon resulting in obstruction of a branch of the pulmonary artery is well monitored by X-ray or magnetic resonance imaging. It is often used to investigate new protocols for these diagnostic methods and to test contrast agents [73, 74, 75].

In addition, gelatin sponge has been used as an embolizing particle in rabbits. The size of these embolizing fragments is standardized at $4 \times 4 \times 10$ mm or $2 \times 4 \times 10$ mm [76, 77, 78, 79, 80].

In a study by Zhang et al. [80] while testing the method of dual-energy lung computed tomography for the diagnosis of PE, a model of embolization of the pulmonary artery branches in rabbits using a gelatin sponge was used. New Zealand white rabbits weighing 2–3 kg were used in this study. Four emboli from a gelatin sponge measuring $4 \times 4 \times 10$ mm or $2 \times 4 \times 10$ mm were injected into the right femoral vein of each rabbit. Two hours after embolism, emboli in the lungs were detected in 18 out of 20 rabbits in the experimental group. In the remaining two rabbits, embolizing particles were found in the inferior vena cava.

Thus, rats and rabbits are the main species in which models with non-thrombotic particles are used. Most of the studies simulating PE in rats were devoted to the study of cardiac and vascular remodeling after PE, as well as drugs for the treatment of PE, which did not target blood coagulation or fibrinolytic systems. A specific niche for the use of this type of model in rabbits is the study of X-ray and magnetic resonance images and testing of new contrast agents.

The main advantages of models using non-thrombotic particles are high standardization and repeatability of the results obtained, and simplicity of modeling. However, artificial particles cannot fully simulate important processes occurring during thromboembolism, such as partial or complete biodegradation and release of biologically active substances: endothelin, catecholamines, platelet-derived growth factor, fibrin degradation products.

2.3. Surgical techniques for modeling of PE

Pulmonary artery occlusion can be achieved not only by embolization with thrombotic or non-thrombotic particles, but also by using surgical techniques. A number of studies have described the ligation of one of the pulmonary arteries as a model of PE [81, 82, 83] (Table 4). Since the left lung in the rat consists of only one lobe (in contrast to the four lobes in the right lung) and is accompanied by a significantly lower perfusion volume, the left pulmonary artery is preferred for modeling. This is also facilitated by the more convenient surgical access to the left pulmonary artery.

All studies with this type of model were conducted in rats. This model has a number of significant drawbacks: it poorly reflects the pathophysiology of the thromboembolic process and is irreversible. The experiment with the pulmonary artery ligation also requires specific surgical experience. In this regard, the main purpose of using this type of model is to study the remodeling of the RV after PE [81].

Table 4. Surgery methods of PE modeling.

N ^o	Animal species	Surgery procedure	Aim of work	Study duration	CTEPH pathway possibility	Authors
1	Rats	Permanent ligation of left pulmonary artery	Studying of pulmonary artery occlusion effect on right ventricular afterload	10 min	–	[81]
2	Rats	Permanent ligation of left pulmonary artery	Studying of CTEPH development mechanisms	2 weeks/5 weeks	CTEPH +	[83]
3	Rats	Permanent ligation of left pulmonary artery	Modeling post-obstructive pulmonary hypertension	2 weeks	CTEPH +/- (short observing time)	[82]

Note: CTEPH — chronic thromboembolic pulmonary hypertension.

3. Modeling of CTEPH

CTEPH is one of the most severe complications of PE and is characterized by a persistent increase in pulmonary artery pressure caused by partial or complete lack of thromboemboli lysis. The high fibrinolytic ability of rodent blood plasma significantly complicates the process of CTEPH modeling. Therefore, in addition to PE, factors leading to CTEPH should be modeled using repeated injection of embolizing particles, stabilization of natural thromboemboli to prevent their lysis, suppression of neoangiogenesis and stimulation of aseptic inflammation.

Most researchers agree that the isolated use of native thrombi prepared in vitro in healthy small laboratory rodents cannot cause the formation of CTEPH [50, 84] because the blood plasma of rodents has great fibrinolytic activity.

Nevertheless, in some studies, the isolated use of thrombi or in combination with tranexamic acid provided the necessary effect in the form of a prolonged increase in pulmonary artery pressure. For example, in a study by Zhou et al. [85] a single in vitro intravenous injection of prepared autologous thrombi into SD rats led to an increase in the mean pulmonary artery pressure on the 28th day after modeling. Before administration, thrombotic masses were treated for 10 min over a water bath at 70 °C; the size of the embolizing particles was 1.1 mm \times 2.0 mm. The effectiveness of tranexamic acid as a fibrinolysis inhibitor for stabilizing exogenously introduced thrombi and the formation of CTEPH is controversial, with some studies confirming its value. For example, a series of studies demonstrated the possibility of using this approach for CTEPH modeling [53, 86, 87]. Experiments were performed on SD rats. Blood was collected from the orbital vein using a tube with an inner diameter of 1 mm. Thrombotic masses were formed at room temperature for 24 h. Cylindrical autologous blood clots were cut to achieve 3-mm length thrombi and suspended in saline containing tranexamic acid at a dose of 200 mg/kg of animal body weight. The suspension was injected into the jugular vein of the anesthetized animal at the rate of 0.2 ml/min. The second injection was performed 4 days after the first injection. Hemodynamic analysis, molecular genetics, and histological studies were carried out at 1, 2, and 4 weeks after modeling. There was a significant increase in the level of mean pulmonary artery pressure and pulmonary vascular resistance in comparison with healthy animals, and a significant increase in these parameters over time.

Li et al. [88] also used a combination of exogenously prepared autologous blood clots with tranexamic acid. During the simulation, rats received three intravenous injections of autologous thromboemboli at 2-week intervals. Each injection included the administration of fifteen 3×1 mm embolizing particles suspended in 2 ml of saline at an administration rate of 0.5 ml/min. During the entire simulation period, tranexamic acid was injected intraperitoneally at a dose of 12.5 mg/kg per day. Four weeks after modeling according to the authors' data, there was a significant increase in systolic pressure in the RV according to cardiac catheterization data, as well as an increase in the ratio of the RV area to the area of the left ventricle according to histological examination.

A similar protocol was used in the previous study by Runyon et al. [50], in which thromboemboli were prepared in vitro in combination

with tranexamic acid and did not result in a persistent increase in systolic pressure in the RV in two rat strains. This was associated with rapid lysis of the thromboemboli. Thus, CTEPH models based on single or multiple administrations of prepared *ex vivo* thromboemboli in combination with tranexamic acid in some cases can give the desired result, although this has not been confirmed by all authors who have used this technique.

Recurrent mechanical obstruction of pulmonary artery branches with thromboemboli is typically considered to be a major mechanism of CTEPH development. However, other mechanisms are also discussed. In particular, chronic vascular inflammation in genetically predisposed individuals might contribute to extensive remodeling of pulmonary vascular bed and increased pulmonary vascular resistance [89]. In one of the studies, an attempt was made to reproduce CTEPH by repeated administration of autologous thrombi in combination with tranexamic acid against the background of a systemic inflammatory response induced by the administration of carrageenan at a dose of 20 mg/kg [90]. In support of the inflammatory theory of CTEPH pathogenesis, the authors observed a more significant increase in pulmonary artery pressure and a more intense remodeling of the pulmonary arteries in the group of animals treated with carrageenan.

As discussed above, blood plasma in rodents is characterized by an outstandingly high fibrinolytic activity, which, despite several previously described successful studies, decreases the utility of thromboembolic models of CTEPH. Therefore, non-thrombotic emboli are much more commonly used for CTEPH modeling. For example, Liu et al. [60] intravenously administered polystyrene microspheres of $25 \pm 1 \mu\text{m}$ in size at a dose of $1.3 \times 10^6/100 \text{ g}$ body weight in rats. At subsequent observation points (3 days and 1, 2, 4, 8, and 12 weeks), there was a consistent increase in the mean pressure in the pulmonary artery, the relative thickness of the media in the distal branches of the pulmonary artery, and the severity of RV hypertrophy.

Arias-Loza et al. [61] used embolizing microspheres with a complex structure; a fibrin-collagen coating was applied to polystyrene microspheres with a diameter of $45 \mu\text{m}$ to ensure better adhesion between the particle surface and vascular endothelium. The resulting microspheres at a dose of 1×10^3 microspheres/g of animal weight and thrombin at a dose of $0.0027 \text{ U}/\mu\text{l}$ were injected into the tail vein of anesthetized male Wistar rats. With a one-week interval, the injection of the embolizing mixture was repeated twice, and during the last injection, the dose of microspheres was reduced to 750 microspheres/g of animal weight. Transthoracic echocardiography (TTE) was performed 7 days after the last injection of microspheres, and the hemodynamics of the right heart chambers were studied and histological examination was performed after 9 days. The authors noted a significant increase in systolic pressure in the RV compared with the control, an increase in the level of brain natriuretic peptide, and a decrease in RV systolic function according to TTE data. It should be noted that the presented model reflects pulmonary hypertension against the background of the subacute stage of PE. A longer observation period is required for final CTEPH formation.

Another hypothesis of CTEPH pathogenesis suggests that a decrease in the intensity of angiogenesis after embolization is of great importance in its formation. Normally, the activation of angiogenesis after repeated episodes of embolism can play an important compensatory role since it leads to a decrease in pulmonary vascular resistance. In the study, it was difficult to ensure decreased angiogenesis; however, a solution was found in a study by Neto-Neves et al. [91], in which CTEPH was modeled against the background of administration of the tyrosine kinase blocker SU5416 to rats, which is capable of suppressing the postreceptor signaling of vascular endothelial growth factor. In this study, modeling was carried out on male SD rats weighing 400–420 g. It was observed that the combined single intravenous administration of $85 \mu\text{m}$ polystyrene microspheres at a dose of 97 000/100 g of body weight and SU5416 lead to a stable increase in systolic pressure in the RV within 6 weeks after embolization. Attention was drawn to the fact that the isolated use of microspheres at the indicated dose did not lead to a significant increase in systolic pressure in the RV.

Frey et al. [92] indicated a possible approach to modeling PE with the further development of CTEPH. This study examined the role of splenectomy in the development of CTEPH. In the course of the study, splenectomy was performed in anesthetized mice, and 1 month after that, a ligature was applied to the inferior vena cava below the left renal vein, causing narrowing of the vessel (residual blood flow corresponded to the 5-0 prolene thread diameter). On the 28th day, the thrombi that formed below the ligature in the group without splenectomy had almost completely resolved, while thrombus lysis in splenectomized animals was significantly delayed. The authors pointed out that the increase in thrombus volume after splenectomy was associated with platelet activation, and the subsequent delay in thrombus resolution was due to inhibition of thrombus recanalization. Thus, although this study did not directly simulate PE, it disclosed a possible approach for the development of new models, reflecting one of the particular clinical variants for CTEPH formation.

Considering the clinical scenario of CTEPH, one may conclude that it is critical to ensure a delayed but controlled pattern of degradation of emboli after repetitive embolic occlusion of segmental/subsegmental branches of the pulmonary artery to develop a successful model of CTEPH. This goal has not been completed by previous studies [93] because the majority of thrombotic emboli are dissolved soon after their administration, while synthetic emboli, such as polystyrene, are not degradable. To circumvent this problem, we suggest the use of partially biodegradable sodium alginate microspheres for modeling CTEPH. Sodium alginate is a natural biopolymer derived from brown algae with high biocompatibility. In previous studies, this polymer was actively used to encapsulate cells of various origins, including beta cells of the Langerhans islets [94] and stem cells [95] with their subsequent implantation into the body. In our study, acellular sodium alginate microspheres have been repeatedly administered in the tail vein in rats for induction of CTEPH. It has been shown that 6 weeks after the last injection of microspheres, there was a decrease in exercise tolerance according to the treadmill test, a significant increase in systolic pressure in the RV and endothelin-1 levels, enlargement of the pulmonary trunk and outflow tract of the RV according to TTE, and remodeling of the pulmonary artery branches according to the histological examination data (Figure 1).

Due to the partial and controlled biodegradation of microspheres and high biocompatibility, sodium alginate is a promising material for the manufacture of embolizing particles in CTEPH simulation. An additional advantage of using sodium alginate microspheres is the possibility of encapsulating a thrombotic mass with the effect of a delayed release of biologically active substances secreted by platelets (serotonin, beta-thromboglobulin, thrombospondin, calcium ions, etc.) and fibrin degradation products, which makes it possible to further improve the compliance of pathogenesis with simulated pathology.

In a study, ligation of the left pulmonary artery was used as an approach to CTEPH modeling [83]. The authors noted a stable increase in systolic pressure in the RV at 2 and 5 weeks after ligation. However, it should be pointed out that this modeling approach seems to be overly mechanistic and reflects only the reduction of the vascular bed as one of the links in CTEPH pathogenesis, without taking into account the molecular mechanisms of vasoconstriction mediated through endothelial dysfunction and aseptic inflammation.

Significant obstruction of the branches of the pulmonary artery in PE is accompanied by high mortality due to acute afterload on the RV. In many patients, CTEPH is formed with recurrent PE, which leads to a significant reduction in the vascular bed of the pulmonary circulation; however, it allows the RV to adapt to a gradually increasing afterload.

In experimental CTEPH modeling, the repeated injection of embolizing particles was also often used, which increased the total volume of embolized vessels and made it possible to reduce mortality due to a gradual increase in right ventricular afterload [53, 61, 88, 93]. The frequency of administration in this approach varied from 2 [53,87] to 8 [93]. In addition, to decrease the acute afterload on the RV in PE and

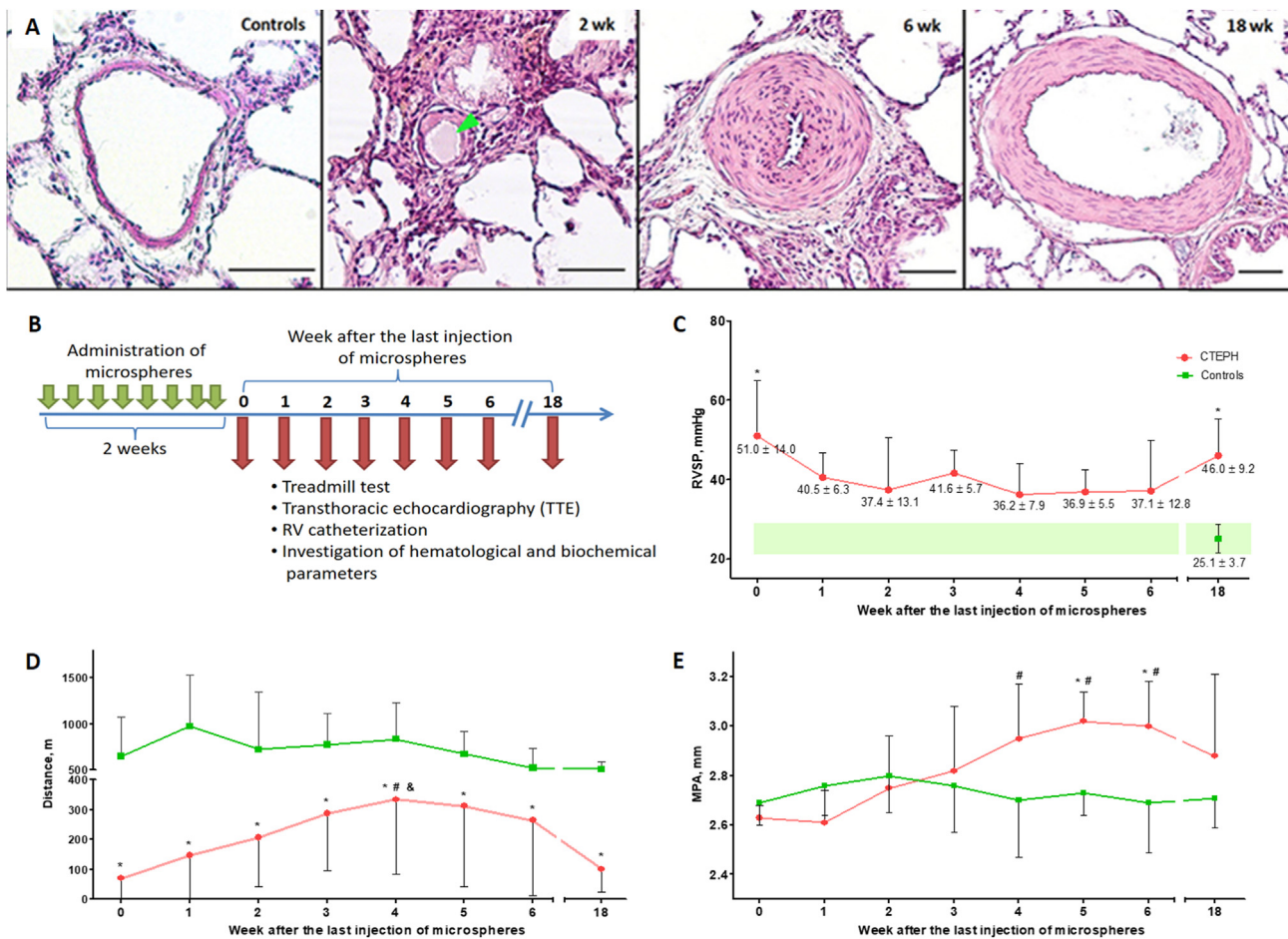


Figure 1. Model of chronic thromboembolic pulmonary hypertension in rats caused by repeated intravenous administration of partially biodegradable sodium alginate microspheres. **A.** Representative microphotographs of the branches of the pulmonary artery by histological examination at different periods of observation after embolization, staining: hematoxylin–eosin, scale bar: 50 μ m, green arrows indicate microspheres in the lumen of the vessels. **B.** Scheme of experiment. **C.** Dynamics of changes in right ventricular systolic pressure (RVSP) at different times after embolization. * $p < 0.05$ in comparison with the control group. **D.** Assessment of exercise tolerance according to the treadmill test. * $p < 0.05$ in comparison with the control group, # $p < 0.05$ in comparison with the 0-week subgroup, and $p < 0.05$ in comparison with the 18-week subgroup. **E.** The diameter of the main pulmonary artery (MPA). * $p < 0.05$ in comparison with the control group. # $p < 0.05$ in comparison with the 0-week subgroup.

prevent the development of acute heart failure, a low injection rate of embolizing particles was used [88].

Thus, at the moment there is no universally accepted CTEPH model. However, despite the complexity of modeling this pathology, over the past ten years, several successful models have been developed, which can be used for preclinical testing of new drugs and for studying the pathogenesis of this pathology. The most common features of CTEPH models are a long observation period (usually more than 4 weeks), repeated administration of embolizing particles, the use of artificial particles resistant to fibrinolysis, or active suppression of the animal's natural fibrinolytic system.

3.1. Species-dependent differences in autonomic innervation of pulmonary vessels and their impact on PE/CTEPH modeling

When choosing the optimal PE model for a number of tasks, it is necessary to consider the specific features of the structure and regulation of the vascular bed of the pulmonary circulation. The most significant interspecies differences are related to innervation.

The pulmonary vascular bed of all mammals is innervated by three types of nerve fibers: sympathetic, parasympathetic, and sensitive. Compared to other organs, the density of innervation and reactivity to vasoactive substances of neuronal origin is highest in large vessels and decreases towards the periphery. In rats and mice, sympathetic and

parasympathetic efferent perivascular axons barely reach the hilum. However, in guinea pigs and rabbits, as in humans, this innervation extends to small intrapulmonary vessels [96, 97].

Thus, rabbits and guinea pigs are the preferred species from those considered in this review for studying the autonomic nervous system. However, one should also consider the complexity of modeling certain variants of PE and especially CTEPH in these species. This requires an individual approach when choosing the type of animal for a particular study.

3.2. Evaluation methods used to describe the PE and CTEPH models

Today, taking into account the rapid development of diagnostic methods, there are many methods of verification and assessment of hemodynamics and molecular genetic abnormalities in the experimental modeling of PE and CTEPH. The entire set of assessment methods can be roughly divided into functional, morphological, molecular biology, and biochemistry. In addition, time-based survival estimates have been used in acute models [9, 17, 28] (see Table 5).

The choice of a set of diagnostic methods for a particular study depends on a wide range of parameters: the purpose of the study, the type of animals, the selected model of PE and CTEPH, and the objective capabilities of the laboratory.

The gold standard for determining hemodynamic changes after PE is catheterization of cardiac cavities with manometry; it is more often used

Table 5. Summary of methods used to describe the PE and CTEPH models.

Functional measurements	<ul style="list-style-type: none"> • Exercise tolerance testing (treadmill-test) • Heart catheterization and pressure measurement: <ul style="list-style-type: none"> - RV - LV - PA - Left atrium • Wire myography
Morphological measurements	<ul style="list-style-type: none"> • Histopathological/immunohistochemical examination: <ul style="list-style-type: none"> - Lung - heart • Computed tomography with contrast enhancement • Perfusion scintigraphy
Combination of functional and morphological assessment	<ul style="list-style-type: none"> • Transthoracic echocardiography (TTE) • Pressure-volume (PV) loop • Magnetic resonance imaging
Molecular biology and biochemistry	<ul style="list-style-type: none"> • Serum NT-proBNP • Transcriptomic analysis of the heart and lung • Serum levels of cytokines and growth factors with ELISA • Analysis of cytokine and growth factor expression in the heart and lung: <ul style="list-style-type: none"> - Western blotting - RT-PCR - ELISA (from tissue extracts)

in rats [83, 93] and rabbits [55]. A possible expanding option for cardiac catheterization is the use of catheters with combined pressure-volume transducers, allowing the construction of a pressure-volume-loop [98]. Telemetry technologies are used to continuously record hemodynamic parameters [91].

The use of isolated heart methods [62, 91] and wire myography of the branches of the pulmonary artery [65] allows a detailed study of the functional activity of the structure under study, excluding the influence of external factors.

An important study that allows the assessment of exercise tolerance, thereby determining the functional class of heart failure, is the treadmill test [93]. Most research using this method has been conducted in rats.

Histological examination of the lungs and heart is an integral part of the overwhelming majority of studies. This allows for the most accurate description of morphological changes that occur after PE. In addition to the standard staining with hematoxylin and eosin, dyes specific to connective tissue are also often used in chronic studies: Masson's trichrome [91], Picrosirius red [61, 62], and Azan according to Heidenhain [93]. Immunohistochemistry makes it possible to clarify the localization of specific molecules and cells in the lung and heart tissue, for example, to identify immune cells (CD 68 [62]), assess proliferation in lung tissue (Ki-67 [91]), or search for new targets for the pathogenesis of PE and CTEPH (HIF-1a [60]).

Additional data on the exact localization of the embolus, the features of the macrostructure of the heart, and the pulmonary vascular bed can be provided by *in vivo* imaging methods such as magnetic resonance imaging [73, 75, 77], computed tomography with contrast enhancement [76, 79, 80], and TTE [57, 91]. In addition, ventilation-perfusion or perfusion scintigraphy was used in a number of studies to determine the localization of emboli [79, 80]. The main animal species on which these methods are used are rabbits because of their large size and ease of technological implementation.

A significant advantage of a number of research methods, such as the treadmill test and TTE, is the possibility of their repeated use. It provides an opportunity to assess morphological and functional changes over time in each specific animal.

The models of PE and CTEPH use the whole range of molecular genetic methods available in modern science, including enzyme-linked immunosorbent assay (ELISA) and Western blot of growth factors, cytokines responsible for inflammation and fibrosis in blood plasma and tissue lysate (heart and lung), real-time polymerase chain reaction (RT-PCR) from the tissue of the lung and heart microarray analyses [47, 99]. For example, Deng et al. [86] used Western blot analysis and RT-PCR to

assess changes in the levels of apoptosis factors (FoxO1, Bad, and Bcl-2) and their corresponding mRNAs. Another study [99] compared gene expression changes in mild and severe PE in a rat model using microarray analyses.

For laboratory confirmation of heart failure and assessment of its dynamics, it is possible to use a blood test for the N-terminal pro-brain natriuretic peptide [42].

4. Conclusion

Based on analyses of the publications describing PE modeling presented in this article, some key conclusions can be drawn. First, it is noteworthy that there is no single optimal method for modeling PE and CTEPH. The choice of a specific model and animal species is determined based on the objectives of the proposed study. For example, two kinds of PE models might be recommended for the studies aiming preclinical testing of anticoagulants, antiplatelet agents, and fibrinolytics: i) administration of *in vitro* prepared blood clots in rats; ii) pharmacological induction of thrombi formation in mice. The use of artificial particles in this case is impossible, and the use of rabbits in most of these studies does not meet the considerations of humanity and economic feasibility.

However, in the study of hemodynamic effects, without considering the reasons for the formation of thromboembolism, it is advisable to use artificial particles. Models of this type are easy to perform and provide a more stable hemodynamic result.

Owing to larger size and better spatial resolution, rabbit models of PE seem to be more suitable for testing new diagnostic X-ray- and magnetic resonance-based approaches. In these models, a prominent branch of pulmonary artery is either embolized by artificial particle(s) or occluded by the inflation of intraluminal balloon.

CTEPH modeling is unique and complex because of insufficient understanding of the pathogenesis of the disease and the significant fibrinolytic activity of rodent plasma. Models used to reproduce CTEPH should be characterized by a persistent increase in pulmonary artery pressure and a stable reduction of the vascular bed due to emboli. The observation period in most of the analyzed publications was more than 4 weeks, which confirmed the stability of the reproduced changes in the models used. An important criterion confirming the success of modeling this pathology is a persistent increase in pulmonary vascular resistance, as well as hypertrophic and fibrotic changes in the pulmonary vessels and right ventricle according to histological examination data.

Further improvement of experimental models of PE and CTEPH is critical for a deeper understanding of the pathogenesis of these disorders and for the preclinical development of new drugs to prevent complications and reduce morbidity and mortality.

Declarations

Author contribution statement

All authors listed have significantly contributed to the development and the writing of this article.

Funding statement

This work was supported by the grant from the Ministry of Science and Higher Education of the Russian Federation (agreement 075-15-2020-800).

Data availability statement

Data will be made available on request.

Declaration of interests statement

The authors declare no conflict of interest.

Additional information

No additional information is available for this paper.

Acknowledgements

None.

References

- [1] G.E. Raskob, P. Angchaisuksiri, A.N. Blanco, H. Buller, A. Gallus, B.J. Hunt, E.M. Hylek, A. Kakkar, S.V. Konstantinides, M. McCumber, Y. Ozaki, A. Wendelboe, J.I. Weitz. Thrombosis, A major contributor to global disease burden, *Arterioscler. Thromb. Vasc. Biol.* 34 (2014) 2363–2371.
- [2] A.M. Wendelboe, G.E. Raskob, Global burden of thrombosis: epidemiologic aspects, *Circ. Res.* 118 (2016) 1340–1347.
- [3] S.V. Konstantinides, G. Meyer, C. Becattini, H. Bueno, G.J. Geersing, V.P. Harjola, M.V. Huisman, M. Humbert, C.S. Jennings, D. Jimenez, N. Kucher, I.M. Lang, M. Lankeit, R. Lorusso, L. Mazzolai, N. Meneveau, F. Ni Ainle, P. Prandoni, P. Pruszczyk, M. Righini, A. Torbicki, E. Van Belle, J.L. Zamorano, E.S.C.S.D. Group, 2019 ESC Guidelines for the diagnosis and management of acute pulmonary embolism developed in collaboration with the European Respiratory Society (ERS), *Eur. Heart J.* 41 (2020) 543–603.
- [4] K. Keller, L. Hobohm, M. Ebner, K.P. Kresoja, T. Munzel, S.V. Konstantinides, M. Lankeit, Trends in thrombolytic treatment and outcomes of acute pulmonary embolism in Germany, *Eur. Heart J.* 41 (2020) 522–529.
- [5] P. Lehnert, T. Lange, C.H. Moller, P.S. Olsen, J. Carlsen, Acute pulmonary embolism in a national Danish cohort: increasing incidence and decreasing mortality, *Thromb. Haemostasis* 118 (2018) 539–546.
- [6] M. Riedel, V. Stanek, J. Widimsky, I. Prerovsky, Longterm follow-up of patients with pulmonary thromboembolism. Late prognosis and evolution of hemodynamic and respiratory data, *Chest* 81 (1982) 151–158.
- [7] S. Crikis, X.M. Zhang, S. Dezfouli, K.M. Dwyer, L.M. Murray-Segal, E. Salvaris, C. Selan, S.C. Robson, H.H. Nandurkar, P.J. Cowan, A.J. d'Apice, Anti-inflammatory and anticoagulant effects of transgenic expression of human thrombomodulin in mice, *Am. J. Transplant.* 10 (2010) 242–250.
- [8] C. Zhong, L. Zhang, L. Chen, L. Deng, R. Li, Coagulation factor XI vaccination: an alternative strategy to prevent thrombosis, *J. Thromb. Haemostasis* 15 (2017) 122–130.
- [9] L. Wang, L. Li, Y. Sun, J. Ding, J. Li, X. Duan, Y. Li, V.B. Junyaprasert, S. Mao, In vitro and in vivo evaluation of chitosan graft glyceryl monooleate as peroral delivery carrier of enoxaparin, *Int. J. Pharm.* 471 (2014) 391–399.
- [10] L. Bevilgia, A. Poggi, C. Rossi, M.A. McLane, R. Calabrese, E. Scanziani, J.J. Cook, S. Niewiarowski, Mouse antithrombotic assay. Inhibition of platelet thromboembolism by disintegrins, *Thromb. Res.* 71 (1993) 301–315.
- [11] F.S. Frattani, E.O. Coriolano, L.M. Lima, E.J. Barreiro, R.B. Zingali, Oral antithrombotic effects of acylhydrazone derivatives, *J. Atherosclerosis Thromb.* 20 (2013) 287–295.
- [12] C.M. Teng, C.C. Wu, F.N. Ko, F.Y. Lee, S.C. Kuo, YC-1, a nitric oxide-independent activator of soluble guanylate cyclase, inhibits platelet-rich thrombosis in mice, *Eur. J. Pharmacol.* 320 (1997) 161–166.
- [13] F. Banno, T. Kita, J.A. Fernandez, H. Yanamoto, Y. Tashima, K. Kokame, J.H. Griffin, T. Miyata, Exacerbated venous thromboembolism in mice carrying a protein S K196E mutation, *Blood* 126 (2015) 2247–2253.
- [14] T.P. Fidler, E.A. Middleton, J.W. Rowley, L.H. Boudreau, R.A. Campbell, R. Souvenir, T. Funari, N. Tessandier, E. Boilard, A.S. Weyrich, E.D. Abel, Glucose transporter 3 potentiates degranulation and is required for platelet activation, *Arterioscler. Thromb. Vasc. Biol.* 37 (2017) 1628–1639.
- [15] V.K. Sonkar, P.P. Kulkarni, D. Dash, Amyloid beta peptide stimulates platelet activation through RhoA-dependent modulation of actomyosin organization, *FASEB J* 28 (2014) 1819–1829.
- [16] J. Katada, Y. Takiguchi, M. Muramatsu, T. Fujiyoshi, I. Uno, The in vitro and in vivo pharmacological profiles of a platelet glycoprotein IIb/IIIa antagonist, NSL-9403, *Thromb. Res.* 88 (1997) 27–40.
- [17] S.W. Huang, H.L. Kuo, M.T. Hsu, Y.J. Tseng, S.W. Lin, S.C. Kuo, H.C. Peng, J.C. Lien, T.F. Huang, A novel thromboxane receptor antagonist, nstpbp5185, inhibits platelet aggregation and thrombus formation in animal models, *Thromb. Haemostasis* 116 (2016) 285–299.
- [18] M.F. Hsu, J.H. Young, J.P. Wang, C.M. Teng, Effect of hsien-ho-t'sao (*Agrimonia pilosa*) on experimental thrombosis in mice, *Am. J. Chin. Med.* 15 (1987) 43–51.
- [19] L. He, L.K. Pappan, D.G. Grenache, Z. Li, D.M. Tollefsen, S.A. Santoro, M.M. Zutter, The contributions of the alpha 2 beta 1 integrin to vascular thrombosis in vivo, *Blood* 102 (2003) 3652–3657.
- [20] W. Paul, P. Gresele, S. Momi, G. Bianchi, C.P. Page, The effect of defibrotide on thromboembolism in the pulmonary vasculature of mice and rabbits and in the cerebral vasculature of rabbits, *Br. J. Pharmacol.* 110 (1993) 1565–1571.
- [21] H. Hayashi, H. Kyushiki, K. Nagano, T. Sudo, H. Matsuoka, S. Yoshida, Anopheline anti-platelet protein from a malaria vector mosquito has anti-thrombotic effects in vivo without compromising hemostasis, *Thromb. Res.* 129 (2012) 169–175.
- [22] K.H. Ryu, H.Y. Han, S.Y. Lee, S.D. Jeon, G.J. Im, B.Y. Lee, K. Kim, K.M. Lim, J.H. Chung, Ginkgo biloba extract enhances antiplatelet and antithrombotic effects of cilostazol without prolongation of bleeding time, *Thromb. Res.* 124 (2009) 328–334.
- [23] S. Momi, F. Impagnatiello, M. Guzzetta, R. Caracchini, G. Guglielmini, R. Olivieri, A. Monopoli, P. Gresele, NCX 6560, a nitric oxide-releasing derivative of atorvastatin, inhibits cholesterol biosynthesis and shows anti-inflammatory and anti-thrombotic properties, *Eur. J. Pharmacol.* 570 (2007) 115–124.
- [24] M.R. Rossiello, S. Momi, R. Caracchini, S. Giannini, G. Guglielmini, A. Monopoli, E. Ongini, N. Semeraro, M. Colucci, P. Gresele, A novel nitric oxide-releasing statin derivative exerts an antiplatelet/antithrombotic activity and inhibits tissue factor expression, *J. Thromb. Haemostasis* 3 (2005) 2554–2562.
- [25] P. Maurice, V. Pires, C. Amant, A. Kauskot, S. Da Nascimento, P. Sonnet, J. Rochette, C. Legrand, F. Fauvel-Lafeve, A. Bonnefoy, Antithrombotic effect of the type III collagen-related octapeptide (KOGEOGPK) in the mouse, *Vasc. Pharmacol.* 44 (2006) 42–49.
- [26] H. Mekhfi, F. Belmekki, A. Ziyat, A. Legssyer, M. Bnouham, M. Aziz, Antithrombotic activity of argan oil: an in vivo experimental study, *Nutrition* 28 (2012) 937–941.
- [27] S. Katsumata, M. Nagashima, K. Kato, A. Tachihara, K. Wauke, S. Saito, E. Jin, O. Kawanami, R. Ogawa, S. Yoshino, Changes in coagulation-fibrinolysis marker and neutrophil elastase following the use of tourniquet during total knee arthroplasty and the influence of neutrophil elastase on thromboembolism, *Acta Anaesthesiol. Scand.* 49 (2005) 510–516.
- [28] P.C. Sathler, A.L. Lourenco, C.R. Rodrigues, L.C. da Silva, L.M. Cabral, A.K. Jordao, A.C. Cunha, M.C. Vieira, V.F. Ferreira, C.E. Carvalho-Pinto, H.C. Kang, H.C. Castro, In vitro and in vivo analysis of the antithrombotic and toxicological profile of new antiplatelets N-acylhydrazone derivatives and development of nanosystems: determination of novel NAH derivatives antiplatelet and nanotechnological approach, *Thromb. Res.* 134 (2014) 376–383.
- [29] P. Gresele, S. Momi, M. Berrettini, G.G. Nenci, H.P. Schwarz, N. Semeraro, M. Colucci, Activated human protein C prevents thrombin-induced thromboembolism in mice. Evidence that activated protein c reduces intravascular fibrin accumulation through the inhibition of additional thrombin generation, *J. Clin. Invest.* 101 (1998) 667–676.
- [30] T. Matsuoka, E. Jin, A. Tachihara, M. Ghazizadeh, A. Nakajima, S. Yoshino, Y. Katayama, O. Kawanami, Induction of pulmonary thromboembolism by neutrophil elastase in collagen-induced arthritis mice and effect of recombinant human soluble thrombomodulin, *Pathobiology* 75 (2008) 295–305.
- [31] S.A. Shaya, R.J. Westrick, P.L. Gross, Thrombus stability explains the factor V Leiden paradox: a mouse model, *Blood Adv* 3 (2019) 3375–3378.
- [32] D.M. Sullivan, J.A. Watts, J.A. Kline, Biventricular cardiac dysfunction after acute massive pulmonary embolism in the rat, *J. Appl. Physiol.* (1985) 90 (2001) 1648–1656.
- [33] S.Q. Li, H.W. Qi, C.G. Wu, X.J. Zhang, S.G. Yang, X. Zhao, Z. Wu, Y. Wang, H.P. Que, S.J. Liu, Comparative proteomic study of acute pulmonary embolism in a rat model, *Proteomics* 7 (2007) 2287–2299.
- [34] B.S. Ding, Y.J. Zhou, X.Y. Chen, J. Zhang, P.X. Zhang, Z.Y. Sun, X.Y. Tan, J.N. Liu, Lung endothelium targeting for pulmonary embolism thrombolysis, *Circulation* 108 (2003) 2892–2898.
- [35] H. Wan, Z. Liu, X. Xia, J. Gu, B. Wang, X. Liu, M. Zhu, P. Li, C. Ruan, A recombinant antibody-targeted plasminogen activator with high affinity for activated platelets increases thrombolytic potency in vitro and in vivo, *Thromb. Res.* 97 (2000) 133–141.
- [36] L. Guarneri, A. Molinari, F. Casacchi, E. Pacci, C. Cerletti, G. de Gaetano, A new model of pulmonary microembolism in the mouse, *J. Pharmacol. Methods* 20 (1988) 161–167.

- [37] J.C. Murciano, S. Medinilla, D. Eslin, E. Atochina, D.B. Cines, V.R. Muzykantov, Prophylactic fibrinolysis through selective dissolution of nascent clots by tPA-carrying erythrocytes, *Nat. Biotechnol.* 21 (2003) 891–896.
- [38] P. Carmeliet, J.M. Stassen, I. Van Vlaenderen, R.S. Meidell, D. Collen, R.D. Gerard, Adenovirus-mediated transfer of tissue-type plasminogen activator augments thrombolysis in tissue-type plasminogen activator-deficient and plasminogen activator inhibitor-1-overexpressing mice, *Blood* 90 (1997) 1527–1534.
- [39] S. Singh, A. Houg, G.L. Reed, Releasing the brakes on the fibrinolytic system in pulmonary emboli: unique effects of plasminogen activation and alpha2-antiplasmin inactivation, *Circulation* 135 (2017) 1011–1020.
- [40] W. Hu, R. Narasaki, N. Nishimura, K. Hasumi, SMTP (Stachybotrys microspora triphenyl phenol) enhances clot clearance in a pulmonary embolism model in rats, *Thromb. J.* 10 (2012) 2.
- [41] L. Wang, J. Wu, W. Zhang, Y. Zhi, Y. Wu, R. Jiang, R. Yang, Effects of aspirin on the ERK and PI3K/Akt signaling pathways in rats with acute pulmonary embolism, *Mol. Med. Rep.* 8 (2013) 1465–1471.
- [42] H.R. Lu, H.R. Lijnen, J.M. Stassen, D. Collen, Comparative thrombolytic properties of bolus injections and continuous infusions of a chimeric (t-PA/u-PA) plasminogen activator in a hamster pulmonary embolism model, *Blood* 78 (1991) 125–131.
- [43] M. Dewerchin, H.R. Lijnen, J.M. Stassen, F. De Cock, T. Quertermous, M.H. Ginsberg, E.F. Plow, D. Collen, Effect of chemical conjugation of recombinant single-chain urokinase-type plasminogen activator with monoclonal antiplatelet antibodies on platelet aggregation and on plasma clot lysis in vitro and in vivo, *Blood* 78 (1991) 1005–1018.
- [44] J.X. Zhang, Y.L. Chen, Y.L. Zhou, Q.Y. Guo, X.P. Wang, Expression of tissue factor in rabbit pulmonary artery in an acute pulmonary embolism model, *World J. Emerg. Med.* 5 (2014) 144–147.
- [45] X. Lin, X.X. Liang, J.J. Tang, J.S. Chen, P.X. Qiu, G.M. Yan, The effect of the fibrinolytic enzyme FIIa from *Agkistrodon acutus* venom on acute pulmonary thromboembolism, *Acta Pharmacol. Sin.* 32 (2011) 239–244.
- [46] Z. Zhang, Z. Meng, Y. Wang, Correlations of inhaled NO with the cTnI levels and the plasma clotting factor in rabbits with acute massive pulmonary embolism, *Acta Cir. Bras.* 33 (2018) 664–672.
- [47] Z. Tang, X. Wang, J. Huang, X. Zhou, H. Xie, Q. Zhu, M. Huang, S. Ni, Gene expression profiling of pulmonary artery in a rabbit model of pulmonary thromboembolism, *PLoS One* 11 (2016), e0164530.
- [48] S.Q. Li, J. Yun, F.B. Xue, C.Q. Bai, S.G. Yang, H.P. Que, X. Zhao, Z. Wu, Y. Wang, S.J. Liu, Comparative proteome analysis of serum from acute pulmonary embolism rat model for biomarker discovery, *J. Proteome Res.* 6 (2007) 150–159.
- [49] W. Witt, B. Baldus, P. Bringmann, L. Cashion, P. Donner, W.D. Schleuning, Thrombolytic properties of *Desmodus rotundus* (vampire bat) salivary plasminogen activator in experimental pulmonary embolism in rats, *Blood* 79 (1992) 1213–1217.
- [50] M.S. Runyon, M.A. Gellar, N. Sanapareddy, J.A. Kline, J.A. Watts, Development and comparison of a minimally-invasive model of autologous clot pulmonary embolism in Sprague-Dawley and Copenhagen rats, *Thromb. J.* 8 (2010) 3.
- [51] J. Wan, L.J. Lu, R. Miao, J. Liu, X.X. Xu, T. Yang, Q.H. Hu, J. Wang, C. Wang, Alterations of bone marrow-derived endothelial progenitor cells following acute pulmonary embolism in mice, *Exp. Biol. Med.* 235 (2010) 989–998.
- [52] C. Chun, W. Yang, C. Xueding, Z. Qi, H. Xiaoying, X. Honglei, Y. Fangyou, C. Chan, L. Yuanyuan, Z. Weixi, Y. Dan, Z. Zhoucang, Y. Lehe, D. Cheng, W. Liangxing, Resveratrol downregulates acute pulmonary thromboembolism-induced pulmonary artery hypertension via p38 mitogen-activated protein kinase and monocyte chemoattractant protein-1 signaling in rats, *Life Sci.* 90 (2012) 721–727.
- [53] C. Deng, D. Wu, M. Yang, Y. Chen, C. Wang, Z. Zhong, N. Lian, H. Chen, S. Wu, Expression of tissue factor and forkhead box transcription factor O-1 in a rat model for chronic thromboembolic pulmonary hypertension, *J. Thromb. Thrombolysis* 42 (2016) 520–528.
- [54] X.K. Li, H.R. Lijnen, L. Nelles, B. Van Hoef, J.M. Stassen, D. Collen, Biochemical and biologic properties of rt-PA (K296-G302), a recombinant human tissue-type plasminogen activator deletion mutant resistant to plasminogen activator inhibitor-1, *Blood* 79 (1992) 417–429.
- [55] V.I. Evlakhov, I.Z. Poyassov, E.V. Shaidakov, Peculiarities of blood flow changes in venae cavae during experimental pulmonary embolism, *Bull. Exp. Biol. Med.* 161 (2016) 759–762.
- [56] J.P. Bouchacourt, J. Riva, J.C. Grignola, Pulmonary hypertension attenuates the dynamic preload indicators increase during experimental hypovolemia, *BMC Anesthesiol.* 17 (2017) 35.
- [57] D. Yu, Y. Wang, Y. Yu, Y. Zhong, L. Huang, M. Zhang, L. Hu, X. Liu, Y. Gu, Acute beneficial effects of sodium nitroprusside in a rabbit model of massive pulmonary embolism associated with circulatory shock, *Am. J. Pathol.* 188 (2018) 1768–1778.
- [58] S.J. Burke, A. Annapragada, E.A. Hoffman, E. Chen, K.B. Ghaghada, J. Sieren, E.J. van Beek, Imaging of pulmonary embolism and t-PA therapy effects using MDCT and liposomal iohexol blood pool agent: preliminary results in a rabbit model, *Acad. Radiol.* 14 (2007) 355–362.
- [59] J. Zagorski, J. Debelak, M. Gellar, J.A. Watts, J.A. Kline, Chemokines accumulate in the lungs of rats with severe pulmonary embolism induced by polystyrene microspheres, *J. Immunol.* 171 (2003) 5529–5536.
- [60] W. Liu, Y. Zhang, L. Lu, L. Wang, M. Chen, T. Hu, Expression and correlation of hypoxia-inducible factor-1 α (HIF-1 α) with pulmonary artery remodeling and right ventricular hypertrophy in experimental pulmonary embolism, *Med. Sci. Mon. Int. Med. J. Exp. Clin. Res.* 23 (2017) 2083–2088.
- [61] P.A. Arias-Loza, P. Jung, M. Abesser, S. Umbenhauer, T. Williams, S. Frantz, K. Schuh, T. Pelzer, Development and characterization of an inducible rat model of chronic thromboembolic pulmonary hypertension, *Hypertension* 67 (2016) 1000–1005.
- [62] J.A. Watts, M.A. Gellar, M. Obratsova, J.A. Kline, J. Zagorski, Role of inflammation in right ventricular damage and repair following experimental pulmonary embolism in rats, *Int. J. Exp. Pathol.* 89 (2008) 389–399.
- [63] J.A. Watts, M.A. Gellar, M.B. Fulkerson, J.A. Kline, A soluble guanylate cyclase stimulator, BAY 41-8543, preserves right ventricular function in experimental pulmonary embolism, *Pulm. Pharmacol. Therapeut.* 26 (2013) 205–211.
- [64] J. Zagorski, M.A. Gellar, M. Obratsova, J.A. Kline, J.A. Watts, Inhibition of CINC-1 decreases right ventricular damage caused by experimental pulmonary embolism in rats, *J. Immunol.* 179 (2007) 7820–7826.
- [65] J.A. Watts, M.R. Marchick, M.A. Gellar, J.A. Kline, Up-regulation of arginase II contributes to pulmonary vascular endothelial cell dysfunction during experimental pulmonary embolism, *Pulm. Pharmacol. Therapeut.* 24 (2011) 407–413.
- [66] J. Zagorski, M.R. Marchick, J.A. Kline, Rapid clearance of circulating haptoglobin from plasma during acute pulmonary embolism in rats results in HMOX1 up-regulation in peripheral blood leukocytes, *J. Thromb. Haemostasis* 8 (2010) 389–396.
- [67] G.A. Riegger, P. Hoferer, A new experimental model for measurement of pulmonary arterial haemodynamic variables in conscious rats before and after pulmonary embolism and during general anaesthesia, *Cardiovasc. Res.* 24 (1990) 340–344.
- [68] D.M. Courtney, J.A. Watts, J.A. Kline, End tidal CO(2) is reduced during hypotension and cardiac arrest in a rat model of massive pulmonary embolism, *Resuscitation* 53 (2002) 83–91.
- [69] H.F. Cuenoud, I. Joris, G. Majno, Ultrastructure of the myocardium after pulmonary embolism. A study in the rat, *Am. J. Pathol.* 92 (1978) 421–458.
- [70] J.J. Byrne, The sympathetic nervous system and pulmonary embolism, *AMA Arch. Surg.* 73 (1956) 936–938.
- [71] A.C. Palei, R.A. Zanetti, G.M. Fortuna, R.F. Gerlach, J.E. Tanus-Santos, Hemodynamic benefits of matrix metalloproteinase-9 inhibition by doxycycline during experimental acute pulmonary embolism, *Angiology* 56 (2005) 611–617.
- [72] D.C. Souza-Costa, L. Figueiredo-Lopes, J.C. Alves-Filho, M.C. Semprini, R.F. Gerlach, F.Q. Cunha, J.E. Tanus-Santos, Protective effects of atorvastatin in rat models of acute pulmonary embolism: involvement of matrix metalloproteinase-9, *Crit. Care Med.* 35 (2007) 239–245.
- [73] T.A. Altes, V.M. Mai, T.M. Munger, J.R. Brookeman, K.D. Hagspiel, Pulmonary embolism: comprehensive evaluation with MR ventilation and perfusion scanning with hyperpolarized helium-3, arterial spin tagging, and contrast-enhanced MR, *J. Vasc. Intervent. Radiol.* 16 (2005) 999–1005.
- [74] J.F. Mata, U. Bozlar, J.P. Mugler 3rd, G.W. Miller, S.S. Berr, K.D. Hagspiel, Time-resolved and high-resolution MR in a rabbit model of pulmonary embolism at 7 T: preliminary results, *Magn. Reson. Imaging* 28 (2010) 139–145.
- [75] S.D. Keilholz, U. Bozlar, N. Fujiwara, J.F. Mata, S.S. Berr, C. Corot, K.D. Hagspiel, MR diagnosis of a pulmonary embolism: comparison of P792 and Gd-DOTA for first-pass perfusion MRI and contrast-enhanced 3D MR in a rabbit model, *Korean J. Radiol.* 10 (2009) 447–454.
- [76] X. Chai, L.J. Zhang, B.M. Yeh, Y.E. Zhao, X.B. Hu, G.M. Lu, Acute and subacute dual energy CT findings of pulmonary embolism in rabbits: correlation with histopathology, *Br. J. Radiol.* 85 (2012) 613–622.
- [77] L.J. Zhang, L. Lu, J. Bi, L.X. Jin, X. Chai, Y.E. Zhao, B. Chen, G.M. Lu, Detection of pulmonary embolism comparison between dual energy CT and MR angiography in a rabbit model, *Acad. Radiol.* 17 (2010) 1550–1559.
- [78] L.J. Zhang, Z.J. Wang, L. Lu, B. Chen, G.M. Lu, Feasibility of gadolinium-enhanced dual energy CT pulmonary angiography: a pilot study in rabbits, *Int. J. Cardiovasc. Imag.* 27 (2011) 1069–1080.
- [79] G.F. Yang, X. Yang, L.J. Zhang, H. Zhu, X. Chai, X.B. Hu, Y.X. Hu, G.M. Lu, Pulmonary enhancement imaging with dual energy CT for the detection of pulmonary embolism in a rabbit model: comparison to perfusion planar scintigraphy, SPECT and SPECT-CT modalities, *Acad. Radiol.* 18 (2011) 605–614.
- [80] L.J. Zhang, X. Chai, S.Y. Wu, Y.E. Zhao, X.B. Hu, Y.X. Hu, Y.B. Xue, G.F. Yang, H. Zhu, G.M. Lu, Detection of pulmonary embolism by dual energy CT: correlation with perfusion scintigraphy and histopathological findings in rabbits, *Eur. Radiol.* 19 (2009) 2844–2854.
- [81] M. Fukumitsu, T. Kawada, S. Shimizu, M.J. Turner, K. Uemura, M. Sugimachi, Effects of proximal pulmonary artery occlusion on pulsatile right ventricular afterload in rats, *Circ. J.* 80 (2016) 2010–2018.
- [82] P. Jungebluth, H. Osterreich, P. Macchiarini, An experimental animal model of postobstructive pulmonary hypertension, *J. Surg. Res.* 147 (2008) 75–78.
- [83] X. Yun, Y. Chen, K. Yang, S. Wang, W. Lu, J. Wang, Upregulation of canonical transient receptor potential channel in the pulmonary arterial smooth muscle of a chronic thromboembolic pulmonary hypertension rat model, *Hypertens. Res.* 38 (2015) 821–828.
- [84] A.A. Karpov, N.A. Anikin, D.E. Cherepanov, A.M. Mikhailova, M.V. Krasnova, S.S. Smirnov, N.S. Bunenkov, S.G. Chefu, D.Yu. Ivkin, O.M. Moiseeva, M.M. Galagudza, Model of chronic thromboembolic pulmonary hypertension in rats, caused by repeated intravenous administration of biodegradable microspheres from sodium alginate, *Reg. Blood Circ. Microcirc.* 18 (1) (2019) 86–95 (In Russ.).
- [85] B. Zhou, G. Sun, F. Mei, H. Xu, The effects of low-molecular-weight heparin on lung and pulmonary artery injuries in acute pulmonary embolism rat model via platelet-derived growth factor-beta, *Saudi Pharmaceut. J.* 25 (2017) 564–569.
- [86] C. Deng, Z. Zhong, D. Wu, Y. Chen, N. Lian, H. Ding, Q. Zhang, Q. Lin, S. Wu, Role of FoxO1 and apoptosis in pulmonary vascular remodeling in a rat model of chronic thromboembolic pulmonary hypertension, *Sci. Rep.* 7 (2017) 2270.

- [87] C. Deng, D. Wu, M. Yang, Y. Chen, H. Ding, Z. Zhong, N. Lian, Q. Zhang, S. Wu, K. Liu, The role of tissue factor and autophagy in pulmonary vascular remodeling in a rat model for chronic thromboembolic pulmonary hypertension, *Respir. Res.* 17 (2016) 65.
- [88] C.Y. Li, W. Deng, X.Q. Liao, J. Deng, Y.K. Zhang, D.X. Wang, The effects and mechanism of ginsenoside Rg1 on myocardial remodeling in an animal model of chronic thromboembolic pulmonary hypertension, *Eur. J. Med. Res.* 18 (2013) 16.
- [89] D.T. Matthews, A.R. Hemnes, Current concepts in the pathogenesis of chronic thromboembolic pulmonary hypertension, *Pulm. Circ.* 6 (2016) 145–154.
- [90] D. Wu, Y. Chen, W. Wang, H. Li, M. Yang, H. Ding, X. Lv, N. Lian, J. Zhao, C. Deng, The role of inflammation in a rat model of chronic thromboembolic pulmonary hypertension induced by carrageenan, *Ann. Transl. Med.* 8 (2020) 492.
- [91] E.M. Neto-Neves, M.B. Brown, M.V. Zaretskaia, S. Rezaia, A.G. Goodwill, B.P. McCarthy, S.A. Persohn, P.R. Territo, J.A. Kline, Chronic embolic pulmonary hypertension caused by pulmonary embolism and vascular endothelial growth factor inhibition, *Am. J. Pathol.* 187 (2017) 700–712.
- [92] M.K. Frey, S. Alias, M.P. Winter, B. Redwan, G. Stubiger, A. Panzenboeck, A. Alimohammadi, D. Bonderman, J. Jakowitsch, H. Bergmeister, V. Bochkov, K.T. Preissner, I.M. Lang, Splenectomy is modifying the vascular remodeling of thrombosis, *J. Am. Heart Assoc.* 3 (2014), e000772.
- [93] A.A. Karpov, N.A. Anikin, A.M. Mihailova, S.S. Smirnov, D.D. Vaulina, L.A. Shilenko, D.Y. Ivkin, A.Y. Bagrov, O.M. Moiseeva, M.M. Galagudza, Model of chronic thromboembolic pulmonary hypertension in rats caused by repeated intravenous administration of partially biodegradable sodium alginate microspheres, *Int. J. Mol. Sci.* 22 (2021).
- [94] D. Pipeleers, B. Keymeulen, Boost for alginate encapsulation in beta cell transplantation, *Trends Endocrinol. Metabol.* 27 (2016) 247–248.
- [95] A.A. Karpov, M.V. Puzanov, D.Y. Ivkin, M.V. Krasnova, N.A. Anikin, P.M. Docshin, O.M. Moiseeva, M.M. Galagudza, Non-inferiority of microencapsulated mesenchymal stem cells to free cells in cardiac repair after myocardial infarction: a rationale for using paracrine factor(s) instead of cells, *Int. J. Exp. Pathol.* 100 (2019) 102–113.
- [96] Y. Wang, D. Yu, Y. Yu, W. Zou, X. Zeng, L. Hu, Y. Gu, Potential role of sympathetic activity on the pathogenesis of massive pulmonary embolism with circulatory shock in rabbits, *Respir. Res.* 20 (2019) 97.
- [97] W. Kummer, Pulmonary vascular innervation and its role in responses to hypoxia: size matters, *Proc. Am. Thorac. Soc.* 8 (2011) 471–476.
- [98] M.J. Faber, M. Dalinghaus, I.M. Lankhuizen, P. Steendijk, W.C. Hop, R.G. Schoemaker, D.J. Duncker, J.M. Lamers, W.A. Helbing, Right and left ventricular function after chronic pulmonary artery banding in rats assessed with biventricular pressure-volume loops, *Am. J. Physiol. Heart Circ. Physiol.* 291 (2006) H1580–1586.
- [99] J. Zagorski, J.A. Kline, Differential effect of mild and severe pulmonary embolism on the rat lung transcriptome, *Respir. Res.* 17 (2016) 86.
- [100] H. Chen, D. Liu, L. Ge, T. Wang, Z. Ma, Y. Han, Y. Duan, X. Xu, W. Liu, J. Yuan, J. Liu, R. Li, R. Du, Catestatin prevents endothelial inflammation and promotes thrombus resolution in acute pulmonary embolism in mice, *Biosci. Rep.* 39 (2019).
- [101] A.K. Gupta, B.S. Chopra, B. Vaid, A. Sagar, S. Raut, M.D. Badmalia, Ashish, N. Khatri, Protective effects of gelsolin in acute pulmonary thromboembolism and thrombosis in the carotid artery of mice, *PLoS One* 14 (2019), e0215717.
- [102] V.V. Inamdar, J.C. Kostyak, R. Badolia, C.A. Dangelmaier, B.K. Manne, A. Patel, S. Kim, S.P. Kunapuli, Impaired glycoprotein VI-mediated signaling and platelet functional responses in CD45 knockout mice, *Thromb. Haemostasis* 119 (2019) 1321–1331.
- [103] A. Patel, J. Kostyak, C. Dangelmaier, R. Badolia, D. Bhavanasi, J.E. Aslan, S. Merali, S. Kim, J.A. Eble, L. Goldfinger, S. Kunapuli, ELMO1 deficiency enhances platelet function, *Blood Adv* 3 (2019) 575–587.
- [104] B.R. Branchford, T.J. Stalker, L. Law, G. Acevedo, S. Sather, C. Brzezinski, K.M. Wilson, K. Minson, A.B. Lee-Sherick, P. Davizon-Castillo, C. Ng, W. Zhang, K.B. Neeves, S.R. Lentz, X. Wang, S.V. Frye, H. Shelton Earp 3rd, D. DeRyckere, L.F. Brass, D.K. Graham, J.A. Di Paola, The small-molecule MERTK inhibitor UNC2025 decreases platelet activation and prevents thrombosis, *J. Thromb. Haemostasis* 16 (2018) 352–363.
- [105] M.O. Jessica, R. Fiorella, S. Ocatavio, R. Linnette, L. Nahomy, M.B. Kanth, M. Bismarck, M.T. Rondina, W.A. Valance, Tlt-1-Controls early thrombus formation and stability by facilitating Aiiib3 outside-in signaling in mice, *Int. J. Adv. Res.* 6 (2018) 1143–1149.
- [106] B.K. Manne, P. Munzer, R. Badolia, B. Walker-Allgaier, R.A. Campbell, E. Middleton, A.S. Weyrich, S.P. Kunapuli, O. Borst, M.T. Rondina, PDK1 governs thromboxane generation and thrombosis in platelets by regulating activation of Raf1 in the MAPK pathway, *J. Thromb. Haemostasis* 16 (2018) 1211–1225.
- [107] W. Lee, S. Lee, J. Choi, J.H. Park, K.M. Kim, J.G. Jee, J.S. Bae, Antithrombotic properties of JJI, a potent and novel thrombin inhibitor, *Sci. Rep.* 7 (2017) 14862.
- [108] W. Lee, J. Lee, R. Kulkarni, M.A. Kim, J.S. Hwang, M. Na, J.S. Bae, Antithrombotic and antiplatelet activities of small-molecule alkaloids from *Scolopendra subspinipes mutilans*, *Sci. Rep.* 6 (2016) 21956.
- [109] A.F. Kucheryavenko, A.A. Spasov, A.V. Smirnov, Antithrombotic activity of a new hypoglycemic compound limiglidole in mouse model of cell thrombosis, *Bull. Exp. Biol. Med.* 159 (2015) 41–43.
- [110] K.Y. Lin, G.A. Kwong, A.D. Warren, D.K. Wood, S.N. Bhatia, Nanoparticles that sense thrombin activity as synthetic urinary biomarkers of thrombosis, *ACS Nano* 7 (2013) 9001–9009.
- [111] C.A. Haller, W. Cui, J. Wen, S.C. Robson, E.L. Chaikof, Reconstitution of CD39 in liposomes amplifies nucleoside triphosphate diphosphohydrolase activity and restores thromboregulatory properties, *J. Vasc. Surg.* 43 (2006) 816–823.
- [112] M. Pozgajova, U.J. Sachs, L. Hein, B. Nieswandt, Reduced thrombus stability in mice lacking the alpha2A-adrenergic receptor, *Blood* 108 (2006) 510–514.
- [113] S. Momi, S.C. Pitchford, P.F. Alberti, P. Minuz, P. Del Soldato, P. Gresele, Nitroaspirin plus clopidogrel versus aspirin plus clopidogrel against platelet thromboembolism and intimal thickening in mice, *Thromb. Haemostasis* 93 (2005) 535–543.
- [114] S. Momi, M. Nasimi, M. Colucci, G.G. Nenci, P. Gresele, Low molecular weight heparins prevent thrombin-induced thrombo-embolism in mice despite low anti-thrombin activity. Evidence that the inhibition of feed-back activation of thrombin generation confers safety advantages over direct thrombin inhibition, *Haematologica* 86 (2001) 297–302.
- [115] K. Gomi, M. Zushi, G. Honda, S. Kawahara, O. Matsuzaki, T. Kanabayashi, S. Yamamoto, I. Maruyama, K. Suzuki, Antithrombotic effect of recombinant human thrombomodulin on thrombin-induced thromboembolism in mice, *Blood* 75 (1990) 1396–1399.
- [116] T. Kumada, W.A. Dittman, P.W. Majerus, A role for thrombomodulin in the pathogenesis of thrombin-induced thromboembolism in mice, *Blood* 71 (1988) 728–733.
- [117] H. Chen, Q. Ma, J. Zhang, Y. Meng, L. Pan, H. Tian, miR106b5p modulates acute pulmonary embolism via NOR1 in pulmonary artery smooth muscle cells, *Int. J. Mol. Med.* 45 (2020) 1525–1533.
- [118] X. Peng, J. Li, X. Yu, R. Tan, L. Zhu, J. Wang, R. Wang, G. Gu, Q. Liu, L. Ren, C. Wang, Q. Hu, Therapeutic effectiveness of bone marrow-derived mesenchymal stem cell administration against acute pulmonary thromboembolism in a mouse model, *Thromb. Res.* 135 (2015) 990–999.
- [119] O.A. Marcos-Contreras, K. Ganguly, A. Yamamoto, R. Shlansky-Goldberg, D.B. Cines, V.R. Muzykantov, J.C. Murciano, Clot penetration and retention by plasminogen activators promote fibrinolysis, *Biochem. Pharmacol.* 85 (2013) 216–222.
- [120] T. Nassar, K. Bdeir, S. Yarvovoi, R.A. Fanne, J.C. Murciano, S. Idell, T.C. Allen, D.B. Cines, A.A. Higazi, tPA regulates pulmonary vascular activity through NMDA receptors, *Am. J. Physiol. Lung Cell Mol. Physiol.* 301 (2011) L307–314.
- [121] Y. Shi, Z. Zhang, D. Cai, J. Kuang, S. Jin, C. Zhu, Y. Shen, W. Feng, S. Ying, L. Wang, Urokinase attenuates pulmonary thromboembolism in an animal model by inhibition of inflammatory response, *J. Immunol. Res.* 2018 (2018) 6941368.
- [122] T. Kikuchi, K. Hasumi, Enhancement of plasminogen activation by surfactin C: augmentation of fibrinolysis in vitro and in vivo, *Biochim. Biophys. Acta* 1596 (2002) 234–245.
- [123] J.M. Stassen, H.R. Lijnen, L. Kieckens, D. Collen, Small animal thrombosis models for the evaluation of thrombolytic agents, *Circulation* 83 (1991) IV65–72.
- [124] X. Xu, L. Shi, X. Ma, H. Su, G. Ma, X. Wu, K. Ying, R. Zhang, RhoA-Rho associated kinase signaling leads to renin-angiotensin system imbalance and angiotensin converting enzyme 2 has a protective role in acute pulmonary embolism, *Thromb. Res.* 176 (2019) 85–94.
- [125] G. Lu, Z. Jia, Q. Zu, J. Zhang, L. Zhao, H. Shi, Inhibition of the cyclophilin A-CD147 interaction attenuates right ventricular injury and dysfunction after acute pulmonary embolism in rats, *J. Biol. Chem.* 293 (2018) 12199–12208.
- [126] J.A. Watts, Y.Y. Lee, M.A. Gellar, M.B. Fulkerson, S.I. Hwang, J.A. Kline, Proteomics of microparticles after experimental pulmonary embolism, *Thromb. Res.* 130 (2012) 122–128.
- [127] J.A. Watts, M.A. Gellar, M.B. Fulkerson, J.A. Kline, Pulmonary vascular reserve during experimental pulmonary embolism: effects of a soluble guanylate cyclase stimulator, *BAY 41-8543, Crit. Care Med.* 39 (2011) 2700–2704.
- [128] M. Toba, T. Nagaoka, Y. Morio, K. Sato, K. Uchida, N. Homma, K. Takahashi, Involvement of Rho kinase in the pathogenesis of acute pulmonary embolism-induced polystyrene microspheres in rats, *Am. J. Physiol. Lung Cell Mol. Physiol.* 298 (2010) L297–303.
- [129] A.E. Jones, J.A. Watts, J.P. Debelak, L.R. Thornton, J.G. Younger, J.A. Kline, Inhibition of prostaglandin synthesis during polystyrene microsphere-induced pulmonary embolism in the rat, *Am. J. Physiol. Lung Cell Mol. Physiol.* 284 (2003) L1072–1081.